POSITRON ANNIHILATION SPECTROSCOPY STUDY OF

RUBBER-CARBON BLACK COMPOSITES

By

VINCENT OKELLO JOBANDO

Bachelor of Science, 1999
Moi University, Kenya.

Master of Science, 2002
Miami University, Oxford Ohio.

Submitted to the Graduate Faculty of the
College of Science and Engineering
Texas Christian University
In partial fulfillment of the requirements
for the degree of

DOCTOR of PHILOSOPHY

December 2006

ACKNOWLEDGEMENTS

The author would like to thank the following people who have been instrumental in the progression of this dissertation. Prof C.A.Quarles, my supervisor for his humbleness, guidance, never-ending pieces of advice and above all, his patience during the course of this work. His intellectual insight about nearly everything was just amazing. I am also indebted to Dr. Leszek from Sid Richardson Carbon Black Company for his useful discussions and for providing us with the samples.

I wish to express my sincere heartfelt to all the faculty members in the Physics Department for their guidance and useful criticism during my studies. I wish to thank Dr. Zerda and Dr. Miller for their never ending advice and for giving me a deeper insight about positron annihilation studies. I wish to extend my gratitude to Dr. Graham for being a great graduate advisor during my studies in the department. Thanks also to Dr. Rittby for enlightening me about some of the theoretical concepts about positronium decay. The list is not ending, Dr. Strzhemechny, Dr. Marcum, and all my fellow graduate students; I owe you a lot of respect. I appreciate the help of Mr. Dave Yale from machine shop for helping me with construction of some of the equipment I used. Not to forget Mrs. Marilyn Yates for her motherly attitude towards us students in the physics department and also Sandy for her promptness in making orders whenever we needed office supplies.

Thanks also go to my dear colleague from positron lab, Jingyi Wang for introducing me to the field of positron and positronum theory and also with the help in understanding PAS equipment.

I am deeply thankful to my late brother Patrice Lumumba Jobando and mother Loice Akuno Jobando for inspiring and encouraging me towards higher education. Had it not been for them, I wouldn't have reached this far. Great honor goes also to my late father, Yuda Jobando for his strict discipline towards his children that enabled me reach this far. David Oyatta, my dearest cousin and a lawyer, I owe you a lot due to your financial and brotherly support. Thanks to all my brothers and sisters for being patient with me during my studies. Finally, I have to thank my wife Mary Okello, for being very patient with me, loving and supportive all these days. Loice thanks for teaching Leanne English.

TABLE OF CONTENTS

LIST OF FIGURES

Figure

LIST OF TABLES

Table

I. INTRODUCTION

Rubber materials find their vast utility in virtually all aspects of life. Their usefulness comes as a result of their desirable properties such as low density, strength, optical clarity, good chemical resistance, good electrical insulation, malleability at relatively low temperature and its cheapness. Understanding their behavior and how they interact with other materials is therefore very important.

The basic understanding of the bulk properties of rubber materials and their composites lies in understanding their molecular behavior at a microscopic level. These rubber molecules are large chains which are free to move about due to the presence of free volume holes or internal voids existing within them [1] [2]. Rubber research is primarily focused in trying to understand the relationship between these free volume holes and their effect on the rubber molecular motion. One of the most applied techniques in investigating the behavior of these free volume holes is *Positron Annihilation Spectroscopy* (PAS) [1] [2]. This technique gives information about the internal structure of different phases of matter in atomic scale and is a useful tool for analyzing the bulk of the rubbers, their composites and as well as polymers in general.

The purpose of this research was to investigate the behavior of rubber and rubber-Carbon Black (CB) filled composites subjected to different physical conditions. The bulk of the work was to investigate the evolution of the free volume holes and to determine their overall effect on the rubber sample material. This was after rubber and their composites were subjected to different degradation conditions. The knowledge of these effects from short-term experimental conditions is therefore paramount to the prediction of the long-term behavior of the rubber composites.

The dissertation is organized as follows: In the remaining chapter I, a brief introduction is given to some of the general properties of rubber and rubber-filler composites that are relevant to the subsequent discussions. Chapter II describes the techniques of positron annihilation spectroscopy. Chapter III summarizes theoretical considerations. Chapter IV describes the samples. Chapter V provides a brief review of previous work on rubber and carbon black composites. Chapter VI describes experimental details and data analysis. Chapter VII, the major part of the dissertation, describes and discusses the results of a wide variety of experiments conducted. Finally, chapter VIII summarizes the major conclusions of the work and suggests directions for further research.

I.1 Physical Aging Phenomenon

One of the most interesting phenomena found in glassy polymers as well as in other non-polymeric glassy materials is the so-called physical aging process. It has been known for many years that amorphous glassy materials are not often at thermodynamic equilibrium, and neither are their physical properties [6]. In simple terms, physical aging of amorphous glassy polymers is the gradual change of the mechanical and physical properties with time as a result of the progression of the non-equilibrium polymer glass towards its equilibrium state [7]. In most of its aspects, physical aging can be explained in a straightforward way from the free-volume concept [8] [9]. The basic idea is that the motion of particles in a closely packed system is dictated by the intensity of packing of the system or by the available free volume.

Volume-relaxation studies of glassy materials have indeed revealed that they undergo slow processes, in attempting to establish equilibrium, indicating that even below glass

transition temperature T_g, molecular mobility is not quite zero. Glass transition temperature gives the boundary between two temperature regimes: the rubbery state ($T > T_g$) and the glassy state ($T < T_g$) where T is the room temperature [7]. Below T_g, the material is hard and brittle, while above T_g the material is soft and flexible. The changes that occur in the free volume are usually brought about by the redistribution of the free volume holes [8] [9] as a result of an external stimuli a sample material encounters, which can either be physical or chemical in nature. For example, a change in temperature or just a stress on the sample can greatly affect the internal structure of the sample, leading to either an increase or a decrease in polymer chain mobility which results into the redistribution of the holes.

The rate at which the free volume relaxation process occurs is determined by the segmental mobility M, resulting in the following closed-loop scheme Struik [7]: free volume (v_f) determines segmental mobility M, while M determines the rate, $\frac{dv_f}{dt}$ at which the free volume, v_f changes.

Symbolically:

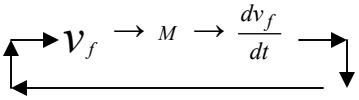

(1)

This closed–loop scheme implies that the volume-relaxation process is non-linear, based on a strong increase in the relaxation time upon free volume reduction Struik [7]. According to this scheme, the differential equation that describes the process of free volume relaxation is

$$\frac{dv_f}{dt} = -\frac{v_f - v_{f\infty}}{\tau(T, v_f)} \tag{2}$$

where $\frac{dv_f}{dt}$ is the aging rate, v_f is the actual free volume, $v_{f\infty}$ is the equilibrium free volume, and τ is the actual relaxation time which is a function of temperature and the free volume. Struik [7] first attempted to describe the relaxation time of this process and proposed a relaxation time equation as a function of both temperature and excess free volume ($v_f - v_{f\infty}$) as:

$$\tau = \tau_o \exp\left\langle \frac{\Delta G}{\kappa \mathrm{T}} - \gamma(v_f - v_{f\infty}) \right\rangle \tag{3}$$

where ΔG is the activation energy which defines the minimum energy needed for this relaxation behavior to occur, κ is gas constant, T is temperature in Kelvin (*K*), τ_o is a pre-exponential factor and is assumed to be independent of T, and γ is a constant. Equation 1 above can best be described by figure 1.1 below [7]. In the first place, it shows that during cooling of amorphous glassy polymer from temperature T_o above T_g to T_1, v_f cannot decrease indefinitely. Below a certain temperature, say T_o, M becomes so small that v_f almost stops decreasing with temperature. The material then passes through its glass transition T_g.Upon further cooling, v_f can only change slightly and slowly. Likewise, M no longer changes rapidly with T, though it continues to decrease slightly because of the decrease in thermal activation (as in fig.1.1; although segmental motion is primarily determined by free volume, it is also thermally activated) after which it is kept at T_1 [10].

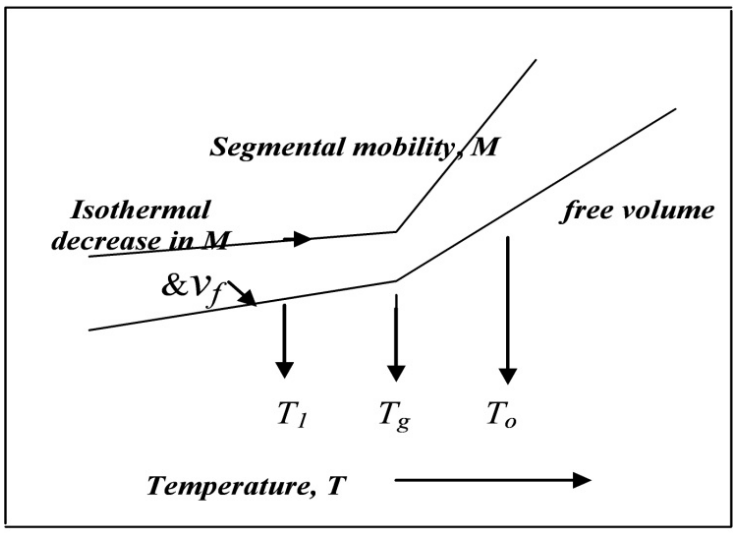

Figure 1.1 The origin of aging explained from the free-volume concept.

Aging can be quantified by changes that occur in volume, length, or color of the sample. In our investigations, we were only concerned about aging effects that comes as a result of volume or length changes in the sample. These changes, when analyzed with appropriate techniques such as PAS directly show the relaxation behavior of the sample. Heat treatment aging for instance is another way of tracing thermal history of the sample and is not limited to glassy polymers. Other polymeric materials such as semicrystalline or filled rubbers also exhibit property-thermal history dependence through physical aging process at temperatures above their glass transition temperatures [7].

Generally, aging mechanisms can be divided into three major groups according to what influences them, namely: physical, mechanical and chemical. Most of the research about aging of natural rubber (NR) has concentrated on the oxidative effects which occur when oxygen attacks the unsaturated bond along the backbone of the NR chain. In this work, we focused mainly on the physical aging mechanisms, though some mechanical

and chemical mechanisms manifested themselves into the physical concept thus were explored. Thermal effects on the properties of NR will be discussed on the context of rubber reversion or degradation and curing.

I.2 Rubber Vulcanization

Rubbers are generally very viscous elastic liquids which can flow, especially at high temperatures. This is because their long molecular chains can slip past each other when under a force. There is a need for one to make bridges among these elastic chains in order to make the rubber behave like a truly elastic material, returning to its original state after being deformed. In that respect, cross-links are introduced between their long molecular chains by reacting rubber with a vulcanizing agent such as sulfur, to form a three-dimensional structure [3]. This reaction changes the weak, soft rubber chains into a strong elastic product. This process is called vulcanization and the cross-linking reaction is illustrated in fig.1.2 below.

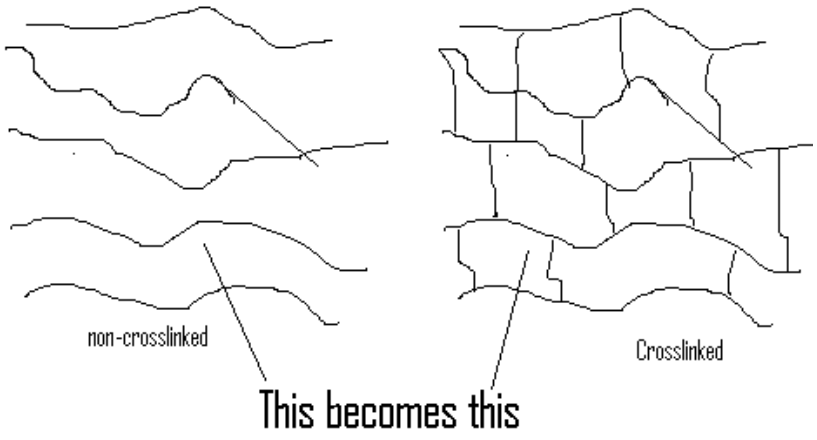

Figure 1.2 Schematic representation of cross-linking

I.3 Rubber Reversion

Rubber reversion refers to the process by which the vulcanized rubber reverts back to its un-vulcanized gum state. This phenomenon has been extensively reviewed by South [11] and only results relevant to the present work will be mentioned here. Huang et al [12] have shown that reversion involves monosulfidic, disulfidic and polysulfidic crosslinks in vulcanized rubber. Lyubchnaskaya et al [13] demonstrated that thermal degradation of polysulfidic bonds is faster than the oxidation of the polymer chain for vulcanizates that do not contain antioxidants. Blackman et al [14] included physical properties in the relation between natural rubber structure and thermal aging. Sloan et al [15] found that reversion was not a linear function of CB loading in rubber CB composites. Finally, Bristow et al [16] showed that the rate of reversion varied by a factor of 1.8 as a function of the grade of CB. Raising the temperature of NR can cause the reversion of the cross-linked sulfur network back to the gum state. This reversion process involves the crosslinks generated during the process of vulcanization and can occur at temperature lower than the NR thermal degradation temperature [12].

I.4 Rubber Molecular Orientation and Crystallization

The orientation of rubber molecules is best studied by either applying stress on a rubber sample or through heat induced crystallization [17] [18]. Other techniques such as stationary fluorescence polarization, FTR and wide angle x-ray scattering [19-20] have also been employed to study these molecular orientations. Rubber vulcanization as already been discussed above involves compounding rubber materials with other ingredients such as sulfur then cured in a mold at high temperature and pressure [3] [5].

Usually a piece of rubber is milled down to a desired thickness and size. The milled sample is then transferred into the mold for curing, changing the sample from a weak viscous material to a strong visco-elastic solid. During milling, the rubber chains can orient themselves in a specific direction making them acquire some molecular orientation history. This milling history can have some effect in a laboratory test results hence during our investigation; we first exposed our samples to the laboratory testing conditions to at least erase the sample's previous thermal history.

Crystallinity in polymer means that certain elements of the polymeric chains have attained a form of three-dimensional order [22] [23]. They possess a certain amount of symmetry and there is a strong accompanying tendency to form ordered domains or crystalline regions, but this crystallinity is never 100% leading to a semi-crystalline structure. The most direct evidence of this fact is provided by x-ray diffraction studies [22]. The x-ray pattern of crystalline polymers shows both sharp features corresponding to regions of three-dimensional order as well as more diffuse features characteristic of molecularly disordered substances like liquids [22]. Additional effects come from other polymer properties, such as density which shows coexistence between crystalline and amorphous structures. According to Whitby et al [23], Natural rubber, for instance, shows some crystalline structure on standing at room temperature or below. They found that maximum crystallization rates occur in the range of -11^{o} C to -35^{o} C. They observed that at 0^{o} C, complete crystallization occurs in 10 days, whereas at -25^{o} C only a couple of hours are required. They also observed that crystallization rates are markedly affected by any stretching of the rubber. At high elongations of the rubber, crystallization can take place within a matter of seconds.

Figure 1.3 below shows the arrangement of polymer chains forming both crystalline and amorphous regions [2]. It can be seen that parts of the molecules are arranged in regular order, usually called crystalline regions. In between these ordered regions, molecules are arranged in a random disorganized state and these are called amorphous regions. Crystallinity is an indication of the amount of crystalline regions in a polymer with respect to the amorphous content [2].

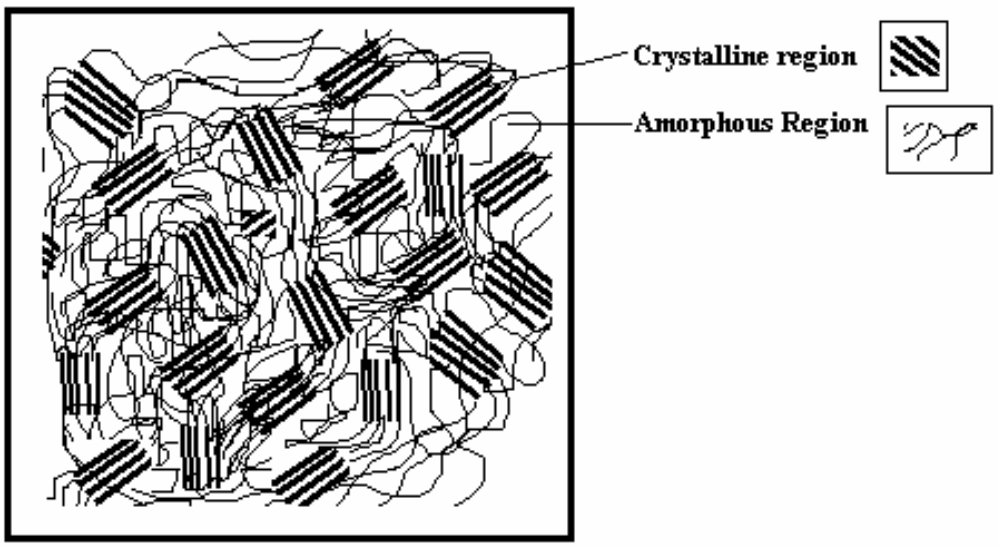

Figure 1.3 Mixed Amorphous Crystalline Polymer Structure

I.5 Rubber Filler Interaction

To reinforce rubber, materials known as fillers are mixed with the rubber sample before vulcanization process is done. Several studies have been performed in trying to understand how rubber interacts with these fillers. For instance, Neogi et al [24] found out that when CB is added to reinforce rubber, the rubber chain mobility is decreased. He attributed this to the interaction and adsorption of the CB particles in the rubber. Wang et al [25] studied the effects between rubber-filler and filler-filler on the dynamic properties

of the vulcanizates. They found that by increasing the amount of carbon black in the rubber sample, the modulus of the compound also increased. Their assertion was that, adsorption of the fillers in the polymer chains occurs thereby restricting the mobility of the polymer segments by forming a rubber shell on the filler surface.

Tamás et al [26] found out that energy of interaction between the polymer and carbon black depends on the nature and population of different sites present on the surface of carbon black.

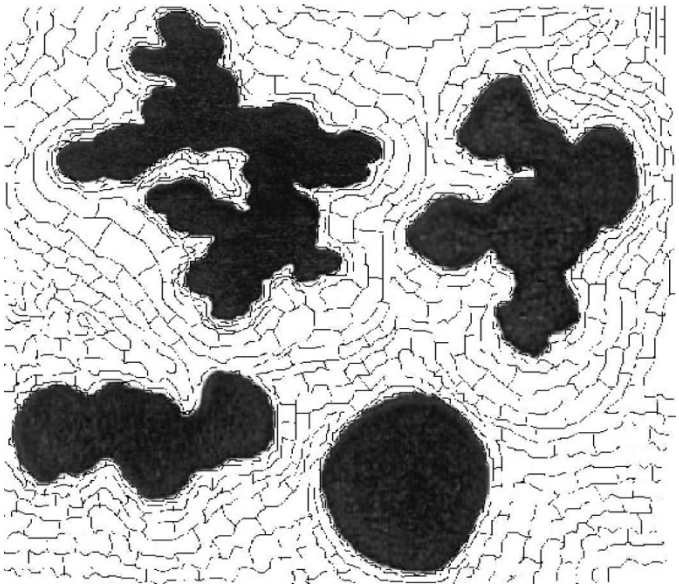

Figure 1.4 Rubber-Carbon Black interaction

They found that the most energetic sites which very effectively adsorb polymers are identified as crystalline flat surfaces. They reasoned that amorphous carbons present on the surface are considered less energetic sites. They also found out that to characterize reinforcing properties of carbon black, it is necessary to determine the fraction of the surface occupied by amorphous carbon and estimate the size of the crystallites with their density.

Figure 1.4 above illustrates this interaction phenomenon between rubber chains and CB aggregates. As has already been discussed, the interaction between the rubber chains and CB aggregates at the vicinity of CB surface is greater as compared to the interaction between rubber chains themselves away from the vicinity of the CB. This is due to the strong Van der Waals forces existing between the CB and rubber chains compared to the weak cohesive forces existing among the chains themselves away from the CB [26]. We therefore expect less rubber molecular chain mobility within the vicinity of CB.

II. POSITRON ANNIHILATION SPECTROSCOPY TECHNIQUE

In our studies, we used positron annihilation spectroscopy (PAS). This unique probe for free volume characterization consists of three different techniques namely: Positron Annihilation Lifetime (PAL), Doppler Broadening Spectroscopy (DBS) and Angular Correlation of Annihilation Radiation (ACAR). In this work, we used mainly PAL and DBS techniques; hence ACAR techniques will not be discussed. However, for interested readers refer to [27] for detailed description of this technique.

II.1 Positron Annihilation Lifetime (PAL)

The basic idea behind this technique is explained in figure 2.1 below [27]. ^{22}Na which is used as a positron source decays to an excited state of ^{22}Ne while emitting the positron. A few ps later a 1274 keV photon is emitted which is used as an indication for the 'birth' of the positron. The positron penetrates into the material, slows down to thermal energies, then diffuses and can get trapped into the defects within the sample. Finally it annihilates with an electron with the emission of two 511 keV photons that are used as an indication for the 'death' of the positron. The time taken from the “birth” of the electron to its death

measures the lifetime of the positron in that material. The following equation is an example of a beta decay involving a ^{22}Na atom;

$$\beta^+ \text{ Decay: } {}^{22}Na \rightarrow {}^{22}Ne + \beta^+ + \upsilon_e + \gamma_{(1.274MeV)} \quad (4)$$

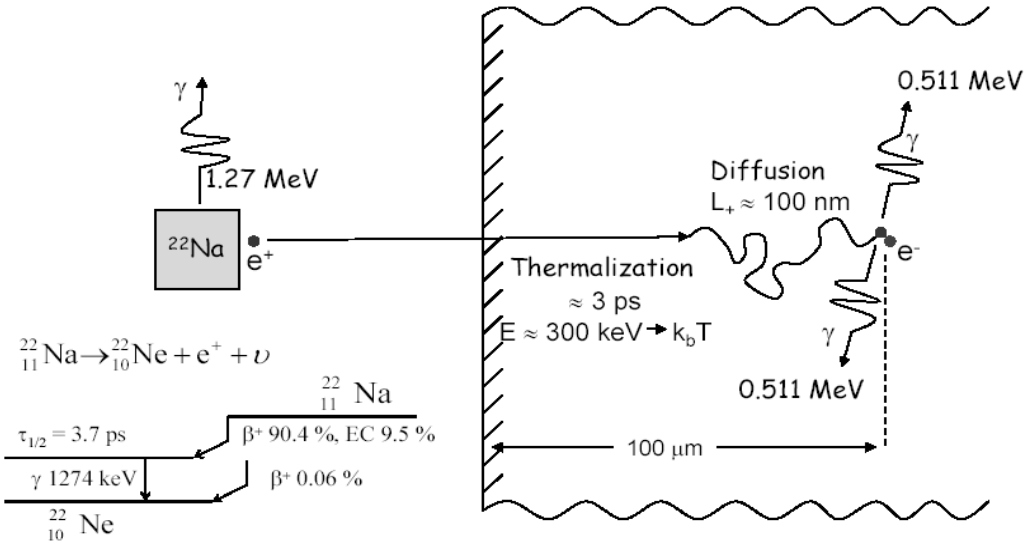

Figure 2.1 Showing Nuclear Decay Scheme of Positron Source ^{22}Na

However, some time during the thermalization process, which happens due to inelastic collisions with ions, electrons or phonons, the positron can do several things: It can annihilate with the surrounding electrons directly emitting the γ-rays; it can localize in a potential well and live longer; or it can form a positronium (Ps), a temporary bound state of the electron and positron [27]. The formation of positronium is very crucial in the studies and understanding of the properties of polymer materials.

The positronium atom is not stable due to the nature of the surrounding molecular medium and the condition the material medium is subjected to. Its lifetime can therefore be shortened, thereby decaying by emitting gamma rays. It has been found to be formed in two spin states: the singlet state called para-positronium (p-P) where the positron and

the annihilating electron have opposite spins having a total spin *S=0;* and the triplet state called ortho-positronium (o-P) where the positron and the annihilating electron have parallel spins with a total spin *S=1*. The p-Ps state has a very short lifetime (about 125 ps in a vacuum) and rapidly annihilates with emission of the two γ-rays at 511 keV. It is presumed to result from the annihilation of either trapped or un-trapped free positrons. On the other hand, o-Ps is a long living system with lifetime of about 142 ns in a vacuum and annihilation occurs with the emission of three γ-rays. In molecular systems, a large fraction of Ps formation is observed in the free-volume regions. The long lifetime of o-Ps gives us a great advantage in quantifying the lifetime results. Since Ps is localized in the free-volume holes, one expects to characterize the material from the measured lifetime. In this case, annihilation occurs after localization of the positron with an electron of opposite spin on the walls of the cavity. This process, known as the *pick-off reaction*, strongly reduces the lifetime of the o-Ps, $\tau_{o\text{-}Ps}$, to values between 2 and 5 ns [2] [27]. The existence of positronium in the polymer is very crucial since it indicates the presence of free volume holes in the polymer. The component of positronium of interest in polymer characterization studies is generally the o-Ps pickoff lifetime component τ_3 and the corresponding intensity I_3.

II.2 Doppler Broadening Spectroscopy (DBS)

DBS provides a sensitive method of defect or free volume characterization by measuring the momentum distribution of the electron-positron pairs at the annihilation site [2]. The principle behind the method lies in the analysis of the positron annihilation line shape, which directly corresponds to the momentum distribution of the electron-positron pairs. The momentum itself is measured from the amount of the Doppler shift of

the emitted photon. If z is the direction of propagation of the emitted photons, then p_z is the momentum component leading to the Doppler shift in the photon energy about the positron/electron rest mass. Since the positron is thermalized in the sample, the momentum is that of the more energetic electron. Two photons are generally emitted due to the conservation of momentum of the positron-electron pair. By employing small angle approximation, the energies of the two photons are approximately given by,

$$E = m_o c^2 \pm \frac{cp_z}{2} \tag{5}$$

where m_o is the electron rest mass.

Since numerous annihilation events are measured to give the complete Doppler spectrum, the energy line of the annihilation is broadened due to the individual Doppler shift in both directions $\pm \frac{cp_z}{2}$ caused mainly by the electron momentum. The spread in the annihilation is characterized by S-parameter which is sensitive to the annihilation with low momentum valence and unbound electrons. This gives information about the momentum distributions of the electrons within the sample which can be used in studying the bulk property of the material. S-parameter is therefore a measure of the amount of positronium formed in the polymer sample material which is used in characterization of the free volume within the sample.

III. SAMPLE

III.1 Elastomers

Elastomers are special types of polymers, and are sometimes called rubbers, having the property of retaining their original shape even after being stretched many times their original length. When a stress is applied to an elastomer, the molecules don't like this and as soon as you remove the stress, the molecules will quickly go back to their entangled disordered state. In our investigations, we focused mainly on the elastomers. There are both natural and synthetic linear elastomeric polymers.

III.1.1 Natural Rubber

Natural rubber has the chemical name of polyisoprene. It is tapped from the bark of a tree of the species *Hevea brasiliensis* as latex [3]. Latex undergoes several processes before it becomes fit for any useful work. One of the main processes it undergoes which is important to this research is vulcanization. As has already been discussed above, vulcanization involves reacting rubber with sulfur or other agents, transforming it to a more usable product [3] [28]. During the vulcanization process, the linear chains of rubber are cross-linked in several places forming a network like structure. The number of cross-links determines the elasticity of rubber. Low sulfur additions leave the rubber soft and flexible, while increasing the sulfur content increases the rigidity of rubber. The main difference between a *vulcanized* rubber and *un-vulcanized* one is that the vulcanized one undergoes heat process in a mold at a temperature of 160^{o} C while the un-vulcanized one does not receive this heat treatment. The chain units of NR consist of same isomer i.e.

same repeat unit making it very regular in structure. This regularity makes natural rubber crystallize upon stretching which results in high gum tensile strength.

III.1.2 Synthetic Rubbers

Synthetic rubbers were developed to supplement the low supply of natural rubber during World War II. They do not have some properties which NR possesses. For instance they do not have the ability to crystallize on stretching; hence they have inferior tensile strength to natural rubber. Mixing them with other reinforcing pigments such as carbon black can make them develop high strengths greater than those of natural rubber. It is believed that the polymer chains form attachments to the surface of these pigments so that the pigment particles act like crystallites in increasing their tensile strength [3]. These synthetic rubbers also undergo vulcanization just like NR. In our investigations, we used D706 synthetic rubber which belongs to the chemical family Butadiene/Styrene Copolymers, generally known as the solution SBR. D706 rubbers have some features superior to natural rubber. They have easily controlled molecular weight with higher concentrations of pure elastomers. They also mix readily with CB and other compounding ingredients and thus readily form a continuous band in milling and extrude smoothly [3].

To achieve maximum vulcanization for these elastomers, several other ingredients have to be added. These are grouped in several categories including:

Accelerators: These materials reduce the vulcanization time (cure time) by increasing the rate of vulcanization. Sometimes, the physical properties of the product are also improved. An example is mercaptobenzothiazole sulfanimide (MBTS).

Activators: These form chemical complexes with accelerators and thus aid in obtaining the maximum benefits from an acceleration system by increasing vulcanization rates and improving the final product's properties. Example is Zinc Oxide (ZnO) or Stearic Acid.

Fillers: These are used to reinforce or modify physical properties of rubbers and to impart certain processing properties or to reduce cost. Example is Carbon Black (CB).

Softeners: These are any materials that can be added to rubber to aid mixing, to promote greater elasticity or tack, or to extend (or replace) a portion of the hydrocarbon (without a loss in physical properties).

III.2 Structure of Rubber

The structure of rubber, just as common polymers shows great variety and complexity as compared to that of metals or ceramics because the building units are not atoms or ions, but macromolecules. The structure is divided into two distinct groups [28] [29]: chemical and physical.

III.2.1 Chemical Structure

Polymers can be *linear, branched* or *cross-linked*. Linear polymers are made up of one long continuous chain without any excess appendages or attachments. The simplest example of a linear polymer is polyethylene. In the chain, the carbon atoms are joined together by covalent bonds. Each carbon atom has four bonds, which are separated by equal 109.5^{o} angles in the space (tetrahedral configuration). The carbon atoms are linked together by single C-C bonds, which allow free rotations preserving the 109.5^{o} tetrahedral

angle. Branched polymers have a chain structure that consists of one main chain of molecules with smaller molecular chains branching from it. Branching prevents dense packing of chains, which therefore reduces the density and strength of the polymer. For example, low-density polyethylene has many branches and is weaker than the high-density polyethylene, which has practically no branching. Cross-linking in polymers occurs when primary valence bonds are formed between separate polymer chain molecules by the cross-linking agent. Most rubbers are either linear or cross-linked [3].

III.2.2 Physical Structure

Segments of a polymer molecule can exist in two distinct physical structures. They can be found in either *crystalline* or *amorphous* forms. Crystalline polymers are only possible if there is a regular chemical structure and the chains posses a highly ordered arrangement of their segments. When macromolecules possess a certain amount of symmetry, there is a strong accompanying tendency to form ordered domains, or crystalline regions as shown in figure 1.3 above. While amorphous polymers, have no order at all in their structure.

III.3 Carbon Black and its Properties.

Carbon black (CB) is an industrial product obtained by partial combustion or thermal decomposition of hydrocarbon compounds [4]. It is mainly produced in the furnace process where feedstock oil, natural gas or other fuel is burned in a non-stoichiometric reaction to form a very finely divided material composed of aggregates that are the CB monounits. Aggregate is the smallest indivisible unit of CB; however, TEM images

reveal that the aggregates appear to be formed by spherical particles which are fused together. Aggregates connect through Van der Waals forces into networks called agglomerates [1] [4]. The internal structure of aggregates is not well understood. Graphite-like, quasicrystalline domains in which basal planes are parallel but angularly distorted with spacing between the layers are different from that of pure graphite. These domains have been detected in CB particles [4]. Biscoe and Warren identified those structures as intermediate between crystalline and amorphous materials. A typical CB aggregate size could range from 50 to 300 nm [3]. Attempts have been made to describe CB in terms of its microstructure, morphology and general physical properties. However, a brief outline of the morphological properties pertinent to these studies will be presented.

There are some physical–chemical properties of CB that play a leading role in the reinforcing ability of CB in rubber which are worth considering [3] [6] [30]. These include:

III.3.1 Surface Area:

Surface area is very important because it determines how much CB surface area is available for interaction with other materials present in a rubber compound. A small particle-size carbon black will have a high surface area accessible for interaction with rubber molecules per unit weight. However, the nature of the surface can also influence the surface area. Surface area is usually measured by adsorption of nitrogen gas on the surface of CB by the BET technique described in reference [31] and is commonly known as N_2SA measurements. Higher N_2SA values mean smaller particle sizes implying more surface area of CB exposed for reaction with rubber and vice versa.

III.3.2 Structure

Structure defines the shape and distribution of the CB aggregates and is sometimes-called aggregate complexity which refers to size, distribution, degree of branching and shape. It gives the degree of irregularity of the CB units or the development of branching due to the aggregation of primary particles and the asymmetry of the aggregates. The

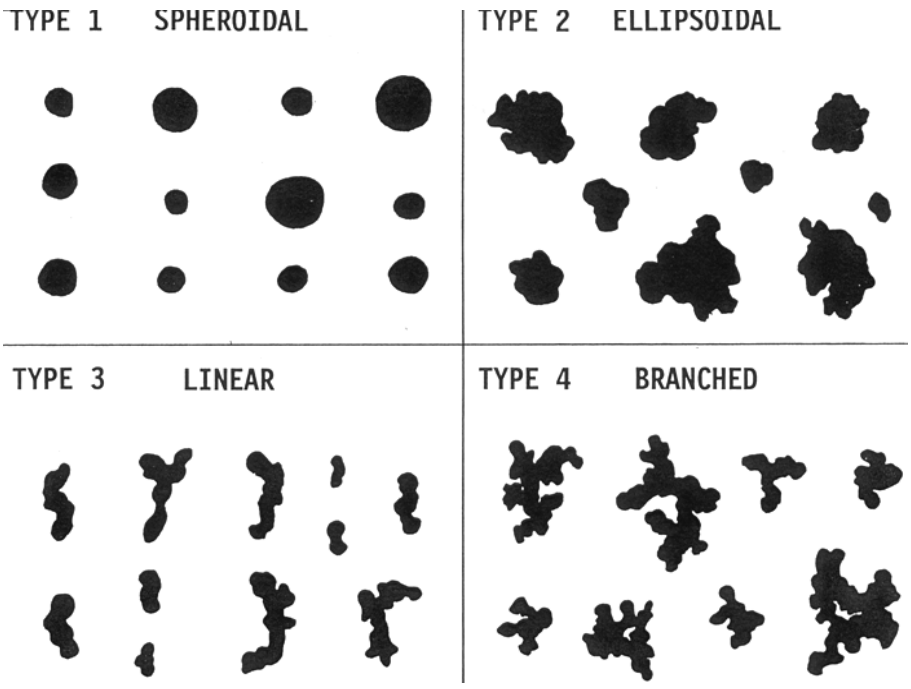

Figure 3.1 Different Structures of Carbon Black

structure is often measured by the amount of DBP (dibutyl phthalate) absorbed by the carbon black original powder and is expressed in ml DBP per 100 g of carbon black. This technique is usually called CDBP and more detailed about it can be found in reference [3]. CB particles with lower CDBP have a more compact, spherical agglomerate structure, while a larger value of CDBP is associated with more flattened, branched particle agglomerate structure. Figure 3.1 and Table 3.1 show different CB shapes and particle sizes respectively. Actually, the amount of adsorbed polymer depends not only

on the surface area, but also on the filler structure. Carbon blacks with same surface area adsorb more or less polymer depending on their aggregate complexity. Therefore, in addition to the effect of carbon black surface area on the interfacial phenomena, one should also consider the contribution of the filler structure as well.

CB	*Tinting Strength (%)*	*Aggregate Diam. (nm)*	*N_2SA (m^2/g)*	*CDBP (g/100g CB)*
N115	123	70	146	94
N135	121	77	71.4	119.5
XLH82	113	85	78.5	109
N326	114	87	79.7	70.1
N358	97	136	79.2	110.6
N772	53	226	27.7	59.8

Table 3.1 Showing a summary of some properties of CB particles

III.3.3 Per hundred of rubber (phr)

Mixtures of rubber compound and carbon black were defined by phr [3]. This defines the amount of CB in grams per 100g of rubber added. This property we used for convenience to distinguish samples, however for other loading studies, we used the amount of filler added in terms of percent by weight.

III.3.4 Chemical Properties and Surface Activity

In a sense, chemical properties and surface are related to the reactivity of the chemical groups on the CB surface. This in a chemical sense is related to the reactivity of the chemical groups on the CB surface. There is evidence for the presence on the surface of at least oxygen-containing groups: carboxyl, phenol, quinine, and lactones. The surface can also differ in adsorptive capacity and in the distribution of sites of high energy [26].

III.3.5 Tinting Strength

Tinting Strength is another way of characterizing CB based on its particle size [4]. In this method, the CB sample is mixed with zinc oxide and a soybean oil epoxide to produce a black or grey paste. This paste is then spread to produce a suitable surface for measuring the reflectance of the mixture with a photoelectric reflectance meter. This reflectance is then compared to the reflectance of paste containing the Industry Tint Reference Black (ITRB) prepared in the same manner. For a given particle size, higher-structure blacks have lower tinting strengths.

The above properties do play a fundamental role in reinforcing rubber through either interfacial interaction between rubber and CB, *occlusion* of the polymer in the internal voids of the aggregate or the agglomeration of CB aggregates in the polymer matrix. These agglomerations form a network held together by Van der Waals forces thereby reinforcing rubber [3] [4] [5].

IV. REVIEW OF PREVIOUS WORK ON RUBBER AND CARBON BLACK FILLED RUBBER.

Polymer is a heavily researched material probably because of its importance in industrial application. Understanding its properties and composites holds a major breakthrough in any future industrial developments. As earlier indicated, its microscopic properties, especially the free volume hole, is of great interest since understanding it is key to understanding its bulk material and behavior.

Marzocca et al [32], for instance, studied the effect on the free volume hole due to cross-linking reaction in a copolymer of styrene butadiene rubber by sulfur vulcanization using PAL. They found out that the free volume size significantly decreased at the onset of the reaction and slightly decreased at high level of cure. They concluded that the presence of cross-links decreased the volume of the holes in the sample, restricting the thermal expansion of the chains.

Salgueiro et al [33] investigated the dependence of physical properties of styrene-butadiene rubber copolymers on the cross-link density by PAL. They found out that glass transition temperature increased while the fractional free volume decreased with increasing sulfur cross-link density. They attributed this to the decrease in hole size by the formation of cross-links per unit volume in the rubber chains.

R. Srithawatpong et al [34] used PAL to study the changes in the free volume on the cross-linking of cis-polyisoprene, polybutadiene and their blends. They found out that there was a decrease in the average size of free volume hole in the rubbery state with increased degree of cross-linking, but no change in the glassy state. They attributed the decrease in the average size of the free volume in the rubbery state to the increase in the packing density of the chains restricted by the cross-linking reaction.

Sung-Seen et al [35] studied the influence of rubber composition on the changes of crosslink density of rubber vulcanizates with efficient vulcanization (EV) cure system by thermal aging. They found that the crosslink densities of the vulcanizates after thermal aging increased continuously with increased aging time.

Deformation studies have also been extensively studied. Jean et al [36] studied anisotropy of the free volume hole dimensions in PEEK (polyaryl-ether-ether-ketone) polymers by PAS. They observed that the free volume hole for unstretched sample was spherical while those of stretched samples were ellipsoidal. They also found out that the average hole radii for unstretched samples were larger than for stretched ones.

G.Dlubek et al [37] studied the local free volume hole in the deformed polyethylene by PAL. They found that the free volume hole size decreased in the amorphous phase of the sample due to a change in the shape of the hole from spherical to ellipsoidal. Wang et al [38] also contributed to the discussion by studying the free volume pressure dependence in amine-cured epoxy polymers by PAL. They observed that the average size and the number of free volume holes decreased with pressure.

The above discussions have concentrated mostly on the general polymers studies. Our interest was in rubber and their composites. One of the earliest few studies in rubber-carbon black composites using PAL as the probing technique was by Mohsen et al [39], who studied the deformation of styrene butadiene carbon black composites. They found four distinct stages during sample deformation. They found that the free volume size and concentrations increased in the first few strokes of deformation and attributed this to the separation of chain entanglements. In the second stage, they observed that the free volume hole size increased while their concentrations decreased, which they interpreted

as filler redistribution process. In the third stage, they observed that the size and the concentrations of the free volume holes decreased and attributed this to the aligning of the chain segments and the redistribution process. Finally, in the fourth stage, they found that the size and the concentrations of the free volume holes only slightly depended on the strain.

In our lab, previous work has been focused mostly on the studies of rubber carbon black composites using PAS method. Quarles et al [40] [41] used the PAL to investigate different carbon black (CB) grades and silica mixed into a variety of rubbers. They found that the o-Ps lifetime did not depend on the filler loading or type of the filler, as shown in figure 4.1 below. They concluded that the free volume which is directly proportional to the o-Ps lifetime is independent of the type of carbon black used. However, they found that the o-Ps intensity which correlates with the number of free volume holes depended on the loading and the type of carbon black used, as shown in figure 4.2 below. They concluded that adding CB decreases the positronium formation by simply providing an additional positron interaction mechanism that competes with the formation of positronium in the rubber. They also argued that if there was not much direct annihilation of the positron in the CB, and because of small CB particle sizes, positron diffused to the CB-rubber interface where they got trapped thereby reducing their chances of forming positronium in the rubber. Hence, this explained why N115 CB with a much larger surface area than N772, gave many more trapping sites with rubber at their interface.

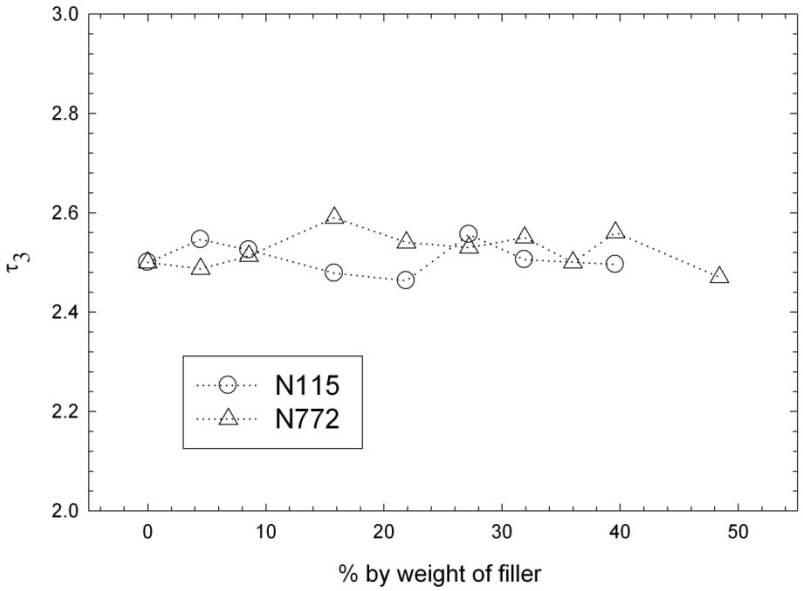

Figure 4.1 The longest o-Ps lifetime versus % by weight of different CB fillers in the same polymer.

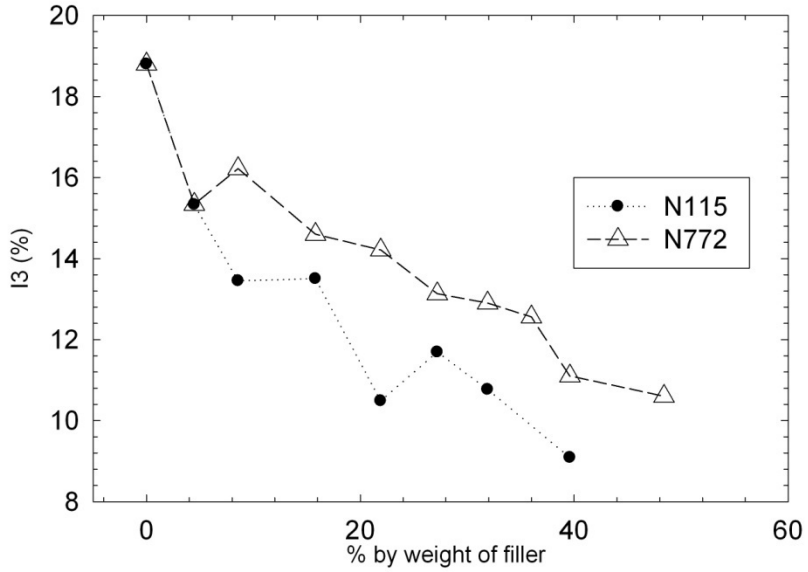

Figure 4.2 The longest o-Ps component versus % by weight of different CB fillers in the same polymer

Semaan et al [42] [43] used DBS to study the effect of loading CB in rubber. They found that the S-parameter which is used in characterization of the annihilation peak decreased with increased loading and also depended on the type of carbon black used.

They also found that S-parameter decreased with CB particle size characterized by N_2SA as well as decrease in S-parameter with CB structure characterized by CDBP. They concluded that S-parameter is sensitive to the structure and morphology of the CB. They further suggested that which was corroborated by Quarles et al that there is a direct correlation between S-parameter and positronium formation which is characterized by o-Ps intensity.

Wang et al [44] [45] also did a comprehensive study on the changes of free volume hole with temperature on carbon black rubber composites as shown in figure 4.3 and figure 4.4. They found that the free volume hole size increased linearly with temperature above glass transition temperature (T_g) and attributed this to the thermal expansion of the polymer chains. They also found that only pure rubber samples

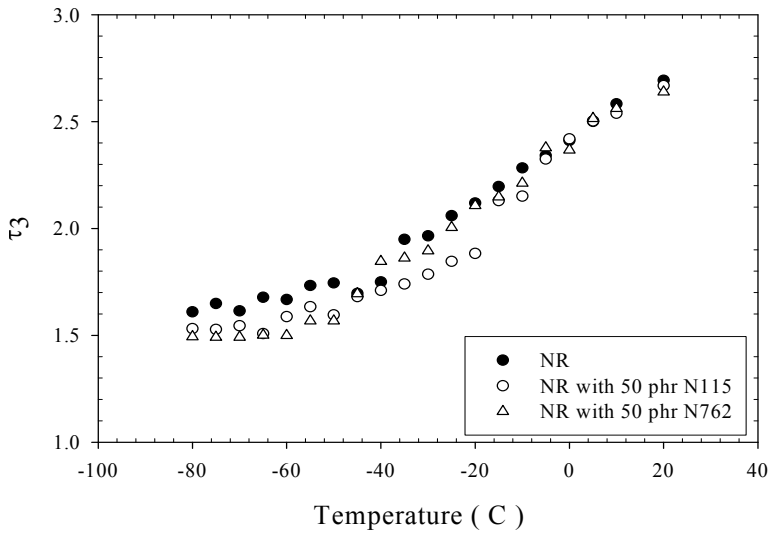

Figure 4.3 Effect of temperature on Natural Rubber–CB composite

exhibited this *phase transition* from the context of the changes in ortho-positronium intensity with temperature, while this phase transition was suppressed in rubber with carbon black.

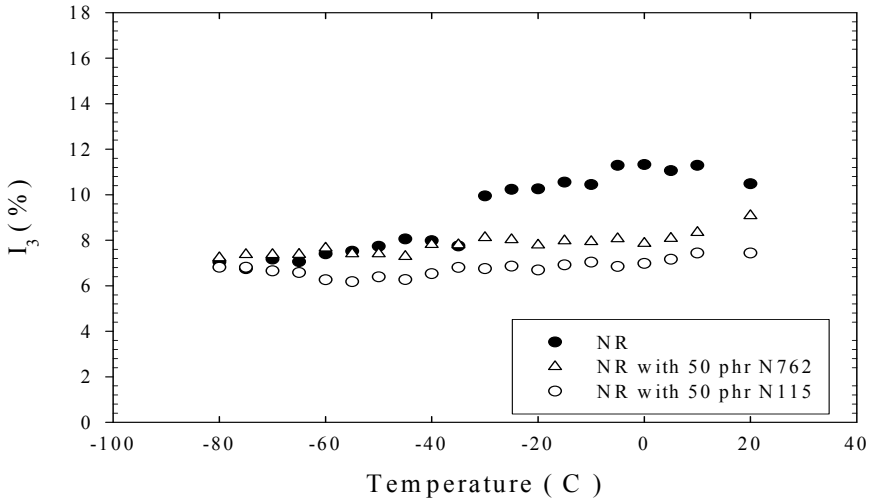

Figure 4.4 Effect of temperature on Natural Rubber–CB composite

As shown in figure 4.5 and Figure 4.6 below, Wang et al also studied the effect of sulfur concentrations in NR-carbon black composites and found that both the number and the size of the free volume holes decreased with sulfur concentrations [44] [45]. They attributed this behavior to the formation of cross-links between sulfur and rubber, which restricted the polymer chains, hence reducing the average free volume hole size and number.

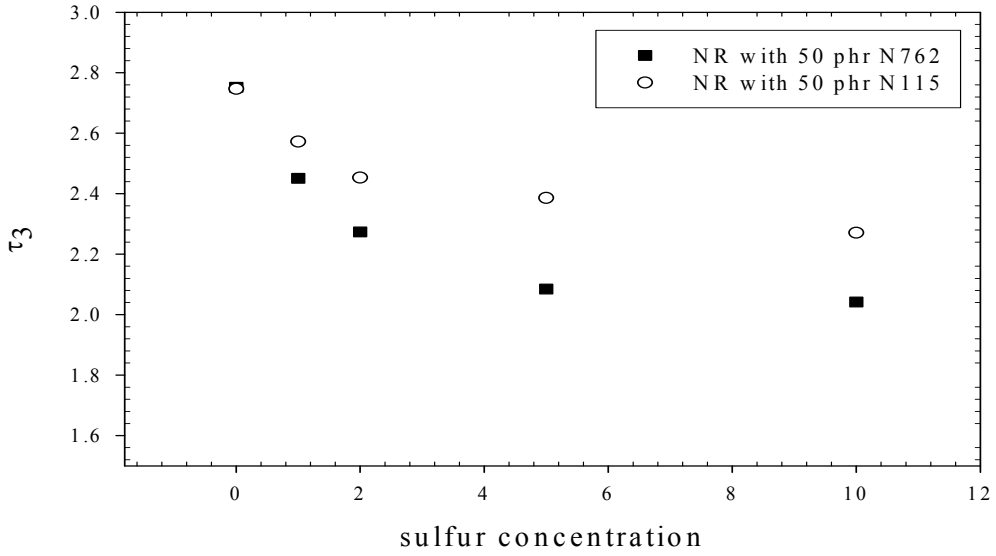

Figure 4.5 o-Ps lifetime, τ_3 vs. sulfur concentration

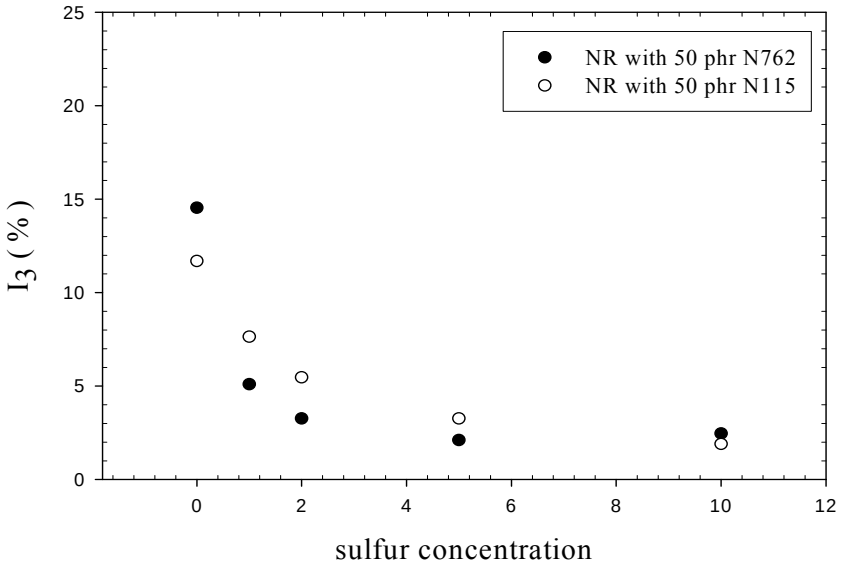

Figure 4.6 o-Ps intensity, I_3 vs. sulfur concentration

Ferrel [46] studied the long lifetime of positronium in liquid Helium. He found that the positronium atom would push Helium atoms away, creating a cavity or a bubble in the liquid. He found that there was very low pickoff rate in liquid helium to the bubble

which formed immediately around each ortho-positronium atom, thereby protecting it from contact with the liquid.

Yu et al [47] used coincidence Doppler broadening to investigate the positronium bubble formation in liquids also. They found that the o-Ps lifetime and intensity for non-polar *n*-hexane and cyclohexane increased from solid to liquid state. They attributed the increase in lifetime to the larger size of Ps bubbles formed in liquids than that of the pre-existing cavities in corresponding solids.

With the above results in mind and much more not reported here, and with the kinds of discrepancies, agreements and observations by the above mentioned investigators, we were motivated to carry out our own investigations. By addressing the discrepancies and our comprehensive review of the above work, we thought we could shed more light on the properties of the rubber materials which have scarcely been studied and hopefully contribute some knowledge to the scientific literature. Also, we wanted to build on the existing research work and extend that which had already been initiated in this lab. A lot of improvements in the performance of rubber materials are continuously being made with the advancement in technology. Our technique is one of the recent methods used in polymer studies availed in the scientific world, and it is therefore worth testing its reproducibility and importance.

V. THEORETICAL CONSIDERATIONS

Relating the motion of matter and the free spaces within them has been long practiced. No motion, even at a microscopic level is possible without an empty space. The search for a relationship between movement of atoms and the free spaces in condensed matter is very interesting to scientists and is one of the motivations in polymer studies.

V.1 Positron and Positronium Chemistry

The process of transforming mass of matter and anti-matter pair into energy is called annihilation while the reverse of the annihilation process is called pair production. [27]. The positron is one of the well-known antimatter particles, (anti-electron for this matter) and was detected by C.D.Anderson in 1932 [49]. The emission of the positron in material medium and the eventual detection of the existence of positronium atom form the back-bone for the use of PAS in polymer research. There are three existing models to describe positronium formation in polymers: Free Volume, Ore and Spur models.

V.1.1 Free-Volume Model

Brandt proposed this model in 1960 and it says that Ps is formed only in an open space of molecular substrates, the so-called Free Volume [50]. It is formed by the positron capturing an electron from the surface of holes or free volumes. This model has been later adopted to describe both the free volume (i.e. dynamic hole in polymers) and hole (i.e. a general term for any open space) properties in polymeric materials as deduced from PAS method. Jean et al [51] [52] quantitatively expressed the free volume which he

defined as an open space that is freely moving in the polymeric material medium as follows:

The free volume (v_f) can be written as the total volume of the polymeric material in question (v_t) minus the occupied volume of the material (v_o):

$$v_f = v_t - v_o \tag{6}$$

He further defined the fraction of the free volume (f_v) in the polymer sample as the ratio of the free volume to the total volume of the material sample:

$$f_v = \frac{v_f}{v_t} \tag{7}$$

This concept has been widely adopted in the community of polymer sciences because it is conceptionally simple and intuitively plausible in understanding many polymer properties at a molecular level.

V.1.2 Ore Model

According to this model, proposed by Ore and Powell in 1949 [53], as the positrons move through the substance due to collisions, they lose most of their energies, becoming slow positrons with energies less than several electron volts in times that are small compared to their lifetimes. During the slowing down process, positrons can capture an electron from the medium substance within a narrow range of kinetic energies (Ore gap or positronium formation gap) to form the atom (e^+e^-), positronium Ps. That is to say, the "hot" positron e^{+*} having some excess kinetic energy pulls out an electron from

molecule M thereby forming a Ps atom, and leaves behind a positively charged radical-cation M^+:

$$e^{+*} + M \rightarrow Ps + M^+ \tag{8}$$

This process is most effective when energy W of the positron lies within the interval named the "Ore gap":

$$I_G - \frac{R_y}{2} < W < W_{ex} or (I_G) \tag{9}$$

I_G is the first ionization potential of the molecule; W_{ex} is its electronic excitation threshold and $\frac{Ry}{2} = 6.8eV$ is the Ps binding energy in vacuum. So a positron with energy lower than $I_G - \frac{R_y}{2}$ cannot pick up an electron from a molecule. When $W > W_{ex}\,(I_G)$ electronic excitations and ionizations dominate and Ps formation become less effective.

V.1.3 Spur Model (Recombination Mechanism)

Mogensen in 1974 [54] proposed that Ps formation would occur through the reaction of a nearly thermalized positron with one of the electrons released by ionization of the medium at the end of the e^+ track, in a small region containing a number of reactive species, like electrons, holes, and excited molecules. This is also referred to as recombination mechanism since the fast e^+ loses most, if not all of its energy on ionization and vibrational excitations and on thermalization, picks up one of the knocked-out intra-track electrons thereby forming a positronium.

V.2 The Bubble Formation

The bubble model was proposed [46] [55] [56] and developed in order to account for the observed increases in the lifetime of ortho-positronium (o-Ps) in liquids for the pickoff reaction process. The physical mechanism underlying the formation of this cavity was thought to be due to the repulsive interaction between o-Ps and the surrounding atoms arising from the electron exchange contribution, which could lead to self-trapped localized state of the positronium as it digs itself a cavity or a bubble in the liquids. The zero-point energy, $(\pi^2\hbar^2)/(4mR_o^2)$ of the positronium atom of mass *2m*, where *m* is the electron mass in an infinitely repulsive spherical well of radius R_o produces a pressure on the bubble wall, balancing the forces of compression due to surface tension of the liquid [46] [55] [56]. Hence in this picture, we expect the surface tension of the surrounding liquid medium to play a leading role in the formation of the bubble. We therefore propose that, the greater the surface tension, the harder it is for the bubble to be formed. This model can be extended to explain some of the results observed in polymer and rubber materials.

V.3 PAS as a Unique Probe for Free-Volume Characterization in Condensed Matter

In the early stages of development, the free volume was merely thought to be a theoretical concept and could not be measured experimentally [36]. This is due to intrinsic difficulties in probing the free volume, which has a size of a few Å and exists at a short time ranging from 10^{-13} s and on. Several techniques, including scanning electron microscopy (SEM) and transmitting electron microscopy (TEM), have been used, but

PAS has proved to be a nanoprobe that has been developed to directly determine the local free-volume hole properties in rubbers and polymeric materials. This technique employs the positron as a probe and monitors its lifetime or that of the positronium in the materials medium under study. Because of the relatively small size of the Ps probe (1.06 Å) compared to other probes, PAS is particularly sensitive to small holes and free volume in a size of Å and at a time of molecular motion from 10^{-10} s and longer. Unlike other methods, PAS is a non-stimulating and non-destructive technique that is sensitive to free volume changes at the molecular level. However, it should be noted that while PAS techniques shed light in understanding many defects in materials at a microscopic level, they have some shortcomings. Due to the broad energy distribution of the positrons resulting from β^+ decay, the penetration depth is also broad and thus these methods are not suitable for investigating near-surface defects or for defect depth profiling. In addition, if the sample is exposed to the source for a considerable amount of time, it may suffer from radiation damage, whereby there is a significant effect on the o-Ps intensity.

In order to understand the experimental PAL parameters, particularly the values of ortho-positronium lifetime (τ_3) and the molecular volumes, it is important to relate the electron and the positron densities to the molecular size. Approximate approaches are feasible at this time. A simple model was proposed by Tao [57] in which a Ps particle resides in a spherical well with radius (R_o) having an infinite potential barrier. The Tao model expresses the o-Ps lifetime as a function of the free volume radius. Hence by knowing the o-Ps lifetime which can be found easily by the LT fitting program in three lifetime mode, one can easily calculate the free volume radius and therefore calculate the free volume hole. For more details on this model, you may refer to the appendix.

A semi-empirical equation has also been developed to determine the fraction of the free volume (f_v) in sample material as

$$f_v = A * V_f * I_3 \tag{10}$$

where V_f is the free volume hole size (in the unit of Angstrom cubed) obtained from τ_3 in equation (38) in the appendix and I_3 (in %) is the o-Ps intensity, and A is a parameter which can be determined by calibrating with other physical parameters, such as specific volume expansion coefficients below and above T_g. For example, in epoxy [51], it has been found that A = 0.0018 by calibrating with the volume expansion coefficients. For polystyrene, it has been found that A = 0.0014 by using the similar method of calibration [58]. In common polymers such as rubber, the value of A ranges from 0.001 to 0.002.

VI. EXPERIMENTAL DETAILS.

VI.1.1 PAL Setup

Our lifetime setup is shown in figure 5.1 below. A ^{22}Na source is sandwiched between two pieces of sample during lifetime measurements. The detectors are Photonis

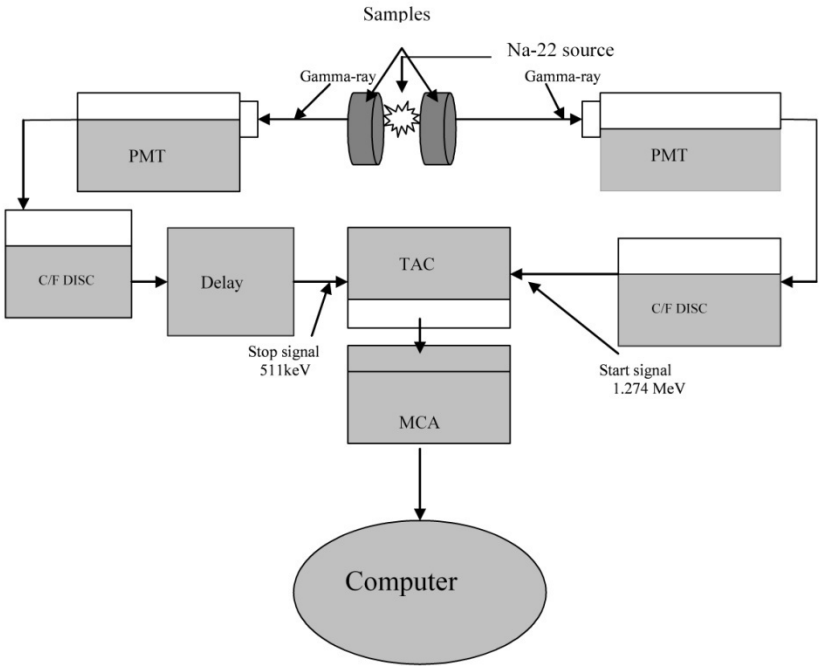

Figure 5.1 PAL experimental setup.

XP2020/URQ photomultipliers coupled to BaF_2 scintillators. The output signals from the photomultipliers are fed to constant fraction differential discriminators (CFDD), which are used to select start and stop signals. One is used to select the 1.274 MeV γ-rays, which accompany the β^+ decay of ^{22}Na, as a start signal for a time-to-amplitude converter (TAC). The other selects a signal around 511 keV as a stop signal for a TAC. The stop signal is delayed by ns-delay (usually 12 ns), to shift the time spectrum into a linear TAC

region in order to get full lifetime spectrum. The output of TAC is then fed onto multi-channel analyzer (MCA) to build up a lifetime spectrum (counts versus time). The spectra from MCA are read out and stored in a PC for analysis by the LT fitting program [48].

VI.1.2 Doppler Broadening Spectroscopy

The scheme for DBS experimental setup is shown in figure 5.2. A high purity germanium detector views the sample in an arrangement with the source between two pieces of rubber sample. The signal from the detector is amplified, recorded in a multi-channel pulse-height analyzer (MCA) and then transmitted to the PC computer for analysis. Liquid nitrogen is used in cooling the detector to reduce the thermal noise in the system.

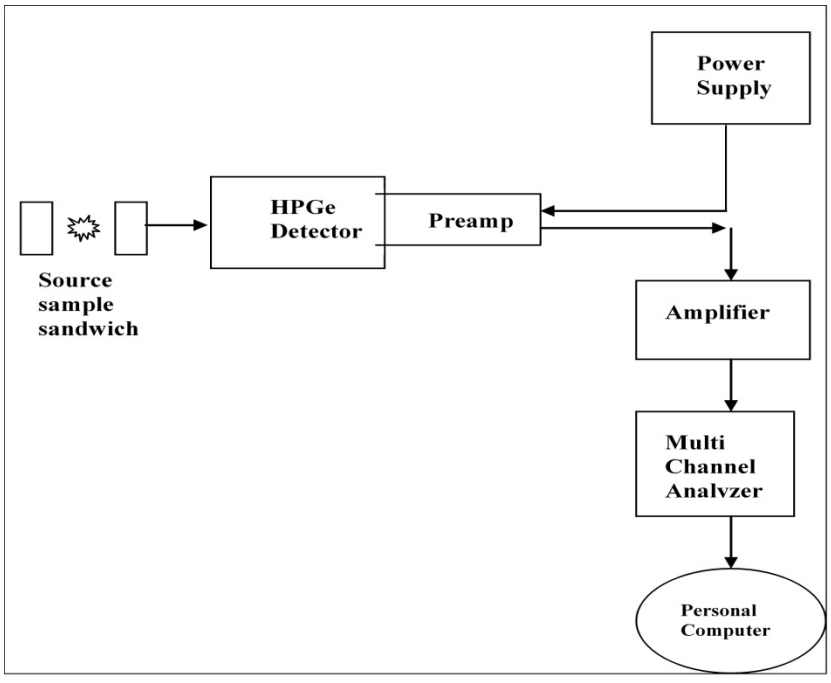

Figure 5.2 Showing a block diagram of a Doppler broadening spectrometer.

VI.1.3 Data Analysis

VI.1.3.1 Positron Annihilation Lifetime Analysis

Once the spectra have been collected, they are analyzed using the LT fitting program with two Gaussian resolution functions and three lifetime components. Each lifetime corresponds to the average annihilation rate of a positron in a different state: the shortest lifetime $(\tau_1 \approx .125ns)$ is due to singlet para-positronium (p-Ps) and is always fixed to stabilize the non-linear fit. This is assumed to result from direct annihilation of the positron with valence or core electrons. The intermediate lifetime ($\tau_2 \approx .40ns$) is due to positrons and positron-molecule species and accounts for the trapping sites of the positron within the sample. The longest lifetime ($1.5 \leq \tau_3 \leq 3.8ns$) is due to triplet ortho-positronium (o-Ps) localized in the free-volume holes. The above lifetimes have their associated intensities I_1, I_2 and I_3 respectively.

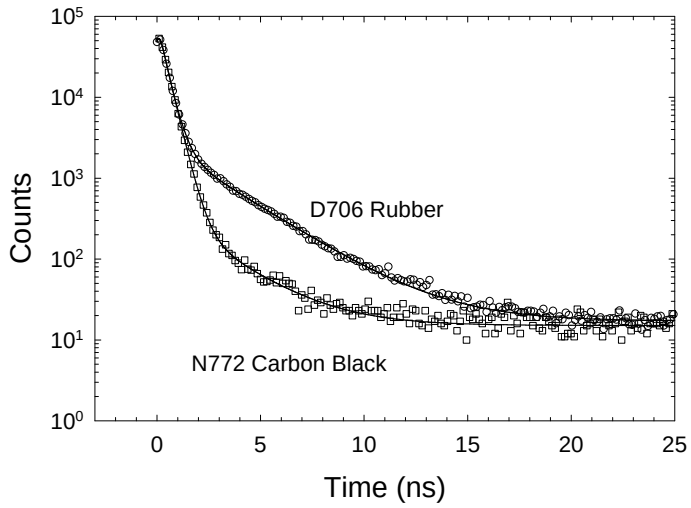

Figure 6.1 A typical Lifetime Spectrum

A positron lifetime spectrum is given by the summation of multi-exponents:

$$N(t) = \sum_{i=1}^{n} I_i e^{-\lambda_i t} \tag{11}$$

The LT program used in the fitting process is based on the mathematical deconvolution as explained below. In a positron annihilation lifetime experiment, the number of positrons *N(t)* remaining in the system at time *t*, can be expressed as an exponential decay:

$$N(t) = \sum_{i=1}^{n} N_{i0} e^{-\lambda_i t} \tag{12}$$

where $\tau_i = \lambda_i^{-1}$ is the lifetime of the i^{th} component. Therefore, in the dt time interval, the event number, $y(t)$ would be,

$$y(t) = dN(t) = \sum_{i=1}^{n} -\lambda_i N_{i0} e^{-\lambda_i t} = \sum_{i=1}^{n} \alpha_i e^{-\lambda_i t} \tag{13}$$

After considering the instrument timing resolution $R(t)$ and constant background, the real response function, $y(t)'$ would be a convolution of $R(t)$ with the event number $y(t)$:

$$y(t)' = \int_{t'=0}^{\infty} y(t') R(t' - t) dt' + B \tag{14}$$

where B is the background.

Assume the timing resolution $R(t - t')$ is a Gaussian distribution,

$$R(t - t') = \frac{1}{\sqrt{2\pi}\sigma} \exp\{\frac{-(t - t')^2}{2\sigma^2}\} \tag{15}$$

After plugging $R(t - t')$ into $y(t)'$ and subtracting background, we obtain the real response function, $y(t)'$ as

$$y(t)' = \sum_{i=1}^{n} \frac{1}{\sqrt{2\pi}\sigma} \int_{t'=0}^{\infty} \alpha_i e^{-\lambda_i t'} \exp\{\frac{-(t-t')^2}{2\sigma^2}\} dt'$$

$$= \frac{1}{\sqrt{2\pi}\sigma} \sum_{i=1}^{n} \alpha_i \int_{t'=0}^{\infty} e^{-\lambda_i t'} \exp\{\frac{-(t-t')^2}{2\sigma^2}\} dt' \quad (16)$$

The data analysis procedure fits the data to the above theoretical response function $y(t)'$, varying the 2n free parameters ($\lambda_i, \alpha_{i,}$ here i is from 1 to n) to minimize the χ^2 function:

$$\chi^2 = \sum_{channels} \frac{[y(t)' - data(t)]^2}{data(t)^2} \quad (17)$$

Here, $y(t)'$ is theoretical response function and $data(t)$ is experimental data.

VI.1.3.2 Doppler Broadening Spectroscopy Analysis

To analyze the DBS spectrum, we used a small Sigma Plot program, which was developed in our lab [59]. Two parameters are used for the interpretation of the DBS spectrum.

S-parameter (shape-parameter)

Shape-parameter defines the ratio of the area under a fixed central part of the peak to the total area of the annihilation peak. It is more sensitive to the annihilation of the low-momentum electrons or valence electrons and its value is usually chosen to be around 0.5. From the peak above, S-parameter can be obtained by

$$S\ Parameter = \frac{Area[I]}{Area[I+III+III]} \tag{18}$$

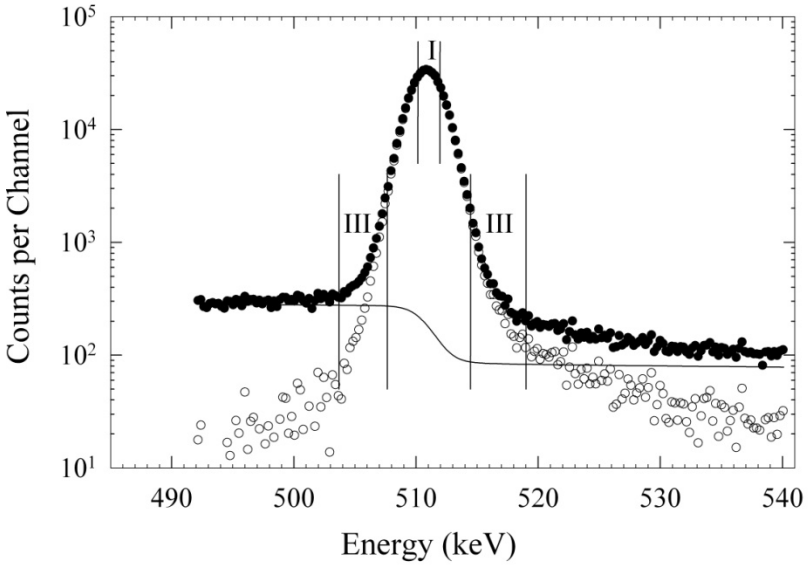

Figure 6.2 Shows the definition of S and W parameter.

W-parameter (Wing parameter**)**

Wing-parameter is computed from the ratio of the area in the edge part of the spectrum to the total area of the peak. Photons, which contribute to the 'wing' part of a spectrum, are created by annihilation with high-energy electrons (core electrons). The range of width is chosen so that W-parameter is approximately 0.25**.** It is defined from the figure by

$$W\ Parameter = \frac{Area[III]}{Area[I+III+III]} \tag{19}$$

VII. RESULTS AND DISCUSSIONS.

This chapter is divided into a series of 8 experimental studies. The first three experiments were done to investigate the sensitivity of the samples to various conditions. First was a radiation test to investigate the sensitivity of the samples to the radiation exposure of the source; second was a study of positronium formation in the vulcanization additives of the rubber samples; and the third was a study of the effect of mixing time on the positron annihilation properties of the sample. The fourth experiment described was a study of the positron annihilation parameters on the surface and structure properties of the CB filler. The fifth experiment was one of the most important results. A comparison of positronium formation, o-Ps intensity and S parameter, for a variety of polymers, liquids and rubbers is described. This study led to the conclusion that rubbers behave more like liquids than polymers below their glass transition temperature and to the use of the bubble model to interpret results of positron formation in rubbers. The sixth experiment describes extensive cross link density measurements using the toluene swelling method. The seventh experiment was a series of studies and curing of the samples. Finally, the eighth experiment is a study of deformation of natural rubber carbon black composites.

VII.1 Radiation Test

One of the major concerns in using PAL as a method of characterizing the polymer materials is the radiation effect. Since the emission of the positron is accompanied by γ-rays, it is expected that these γ-rays or the positrons themselves can cause a lot of damage to the polymer sample material. Most studies have revealed that the o-Ps lifetime is largely unaffected by the prolonged exposure to the positron source. However effects have been found on the o-Ps intensities in some polymers, including polyethylene,

polycarbonates, polystyrene [60-62]. This positron irradiation effect in polymers has been found to strongly depend on time, temperature and the nature of the polymers. Most researchers have found that the decrease in o-Ps intensity on exposure mainly occurs in non-polar or weakly polar polymers. They have attributed this decrease to the build-up of electric field inside the polymer during prolonged PAL measurements [62] [63]. It was therefore important for us to test our samples for any possible irradiation effect in order to help eliminate any potential errors in trying to interpreting our results. To do this, a source was sandwiched between two identical rubber samples and the lifetime measurements were initiated for ten consecutive runs at the same spot. The analysis was done and the o-Ps lifetime and intensities plotted versus run number as shown in figure 7.1 and figure 7.2 respectively.

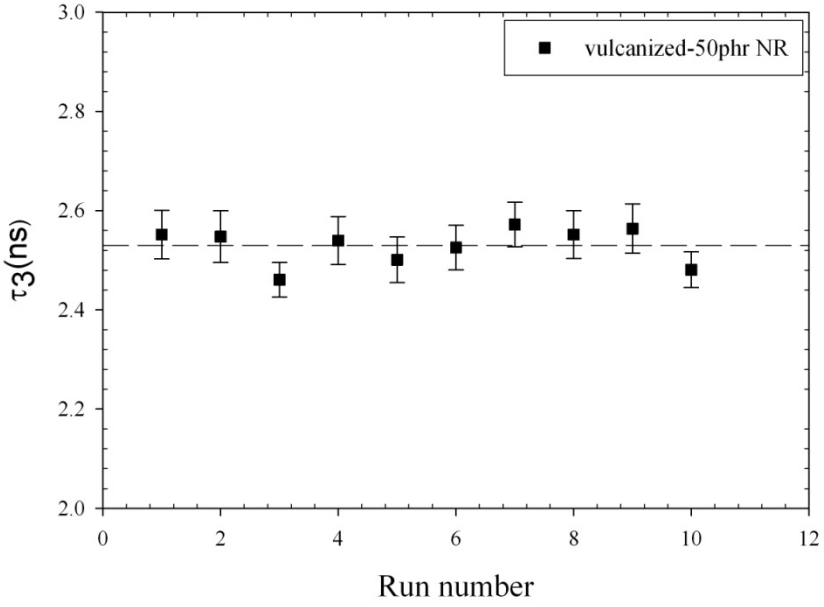

Figure 7.1 The o-Ps Lifetime versus Run Number

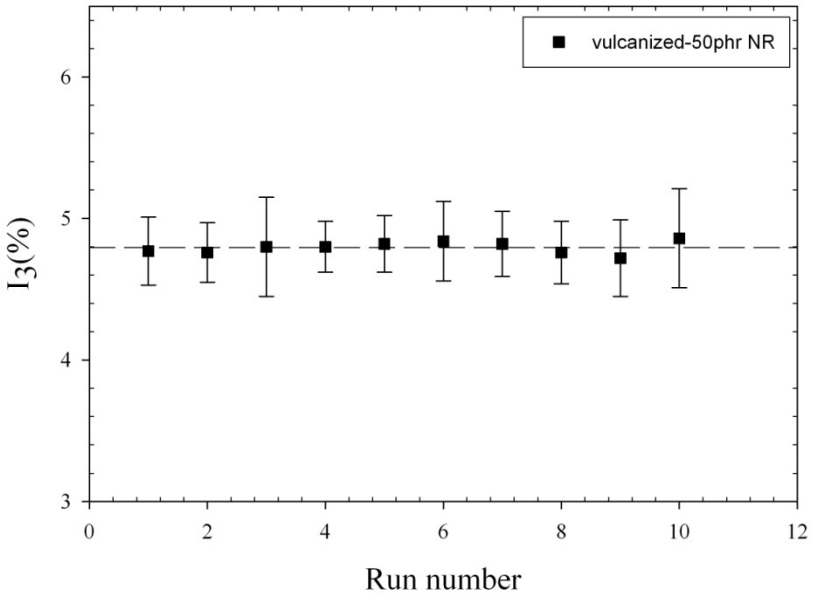

Figure 7.2 The o-Ps Intensity vs. Run Number.

There was no significant change in the o-Ps lifetime and intensities on continued exposure to the positron source as the figures suggest. We concluded that our samples were not affected by our ^{22}Na source, which was originally at 10 μCi.

VII.1.1 Conclusions

The ^{22}Na positron source used in this investigation did not have any effect on our samples.

VII.2 Sensitivity of PALS to Vulcanization Additives

Compounding of NR with additives is done before it is vulcanized [3]. We investigated the sensitivity of PALS to these vulcanization additives, individually before and after heating them at the vulcanization temperature of 160^{o} C. The additive samples were studied in their bulk-powdered forms by sandwiching the positron source between a pair of identical samples placed in sample holders with kapton-foil covers. Our main goal

in performing this test was to check how each of the constituent components in our composites affects the o-Ps formation. The results shown in figure 7.4 below suggest that sulfur, which is the main vulcanization agent, does not form any meaningful positronium in its bulk-powdered state. This could be due to the fact that sulfur itself is considered a metal hence we expect higher electron densities which could favour direct annihilations rather than positronium formation. Any long lifetime observed as shown in figure 7.3, was attributed to impurities.

The other additives, zinc oxide (ZnO) and mercaptobenzothiazole sulfanimide (MBTS), which were used as accelerators in the vulcanization process, also did not show any significant positronium formation before or after heating. Only stearic acid exhibited higher percentage of positronium formation before and after heating, as shown in figure 7.4.

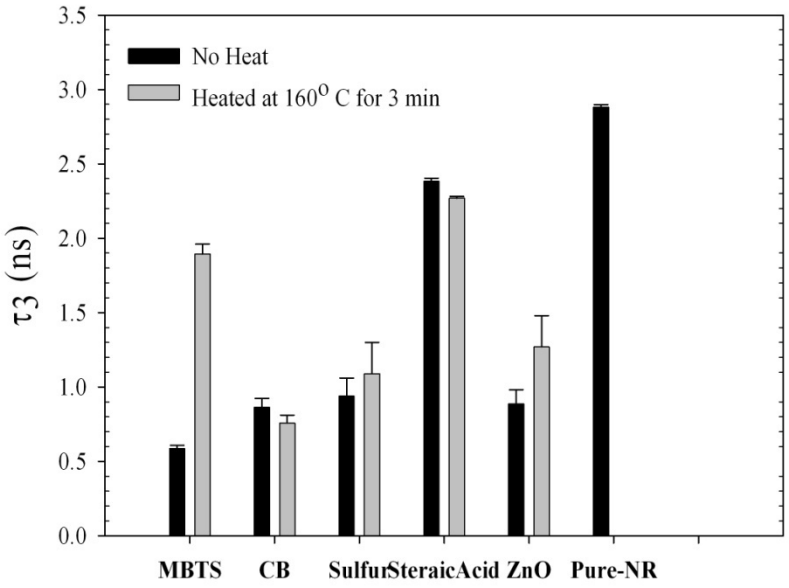

Figure 7.3 The o-Ps Lifetime vs. Vulcanization Additives.

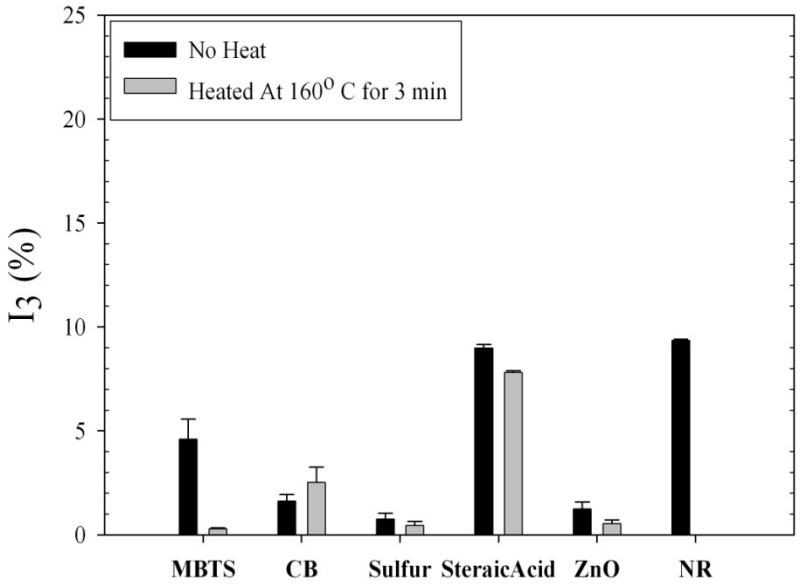

Figure 7.4 The o-Ps Intensity vs. Vulcanization Additives.

VII.3 Mixing Measurements

The mixing of compounds is one of the most complex chemical processes in any aspect of life. Since polymers and their composites form a key raw material for industrial use, any structural abnormalities as a result of the mixing process can be very detrimental and costly as far as the ultimate product is concerned. We investigated whether both PAL and DBS are sensitive to the mixing process as a function of time. We hypothesized that, the longer the mixing time, the more mixed the sample would be and the chances of eliminating any existing free volume holes would increase. The sample we used was un-vulcanized pure Natural Rubber mixed with sulfur, MBTS and Stearic acid. After PAL measurements, the o-Ps lifetime and intensity were plotted as shown in figure 7.5 and 7.6 respectively. A trend line was drawn through the points which suggests no effect of mixing time on the o-Ps lifetime and intensity, as can be observed in figure 7.5 and 7.6.

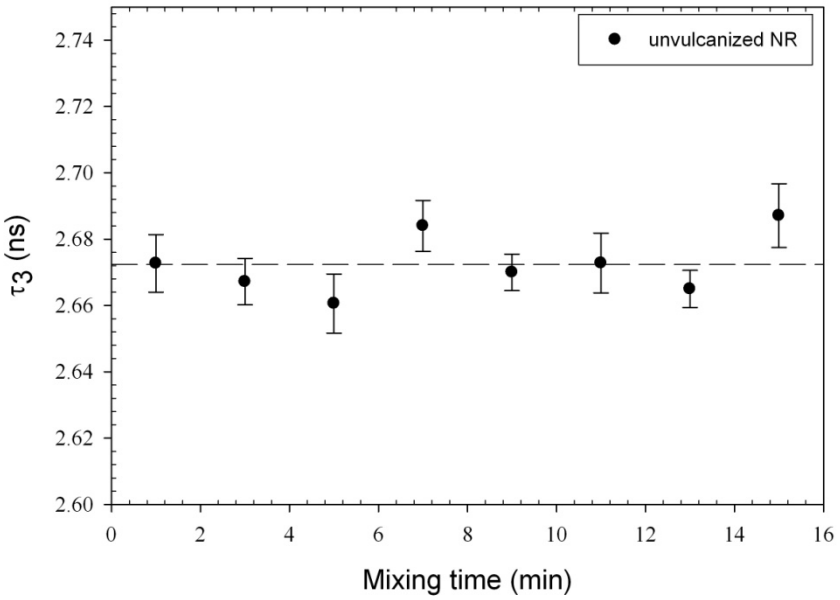

Figure 7.5 The o-Ps Lifetime vs. Mixing Time

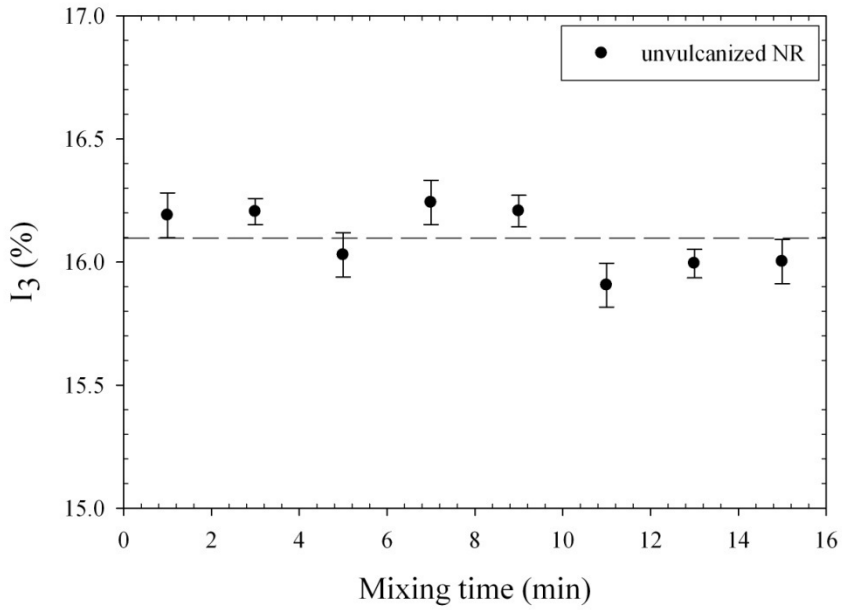

Figure 7.6 The o-Ps Intensity vs. Mixing Time

We also did some DBS measurements on the mixing time and reported the results as shown in figure 7.7 below. This agreed well with the o-Ps intensity observed in figure

7.6, showing that PAS is insensitive to the mixing time. These results are compatible well with what had already been observed by others [43].

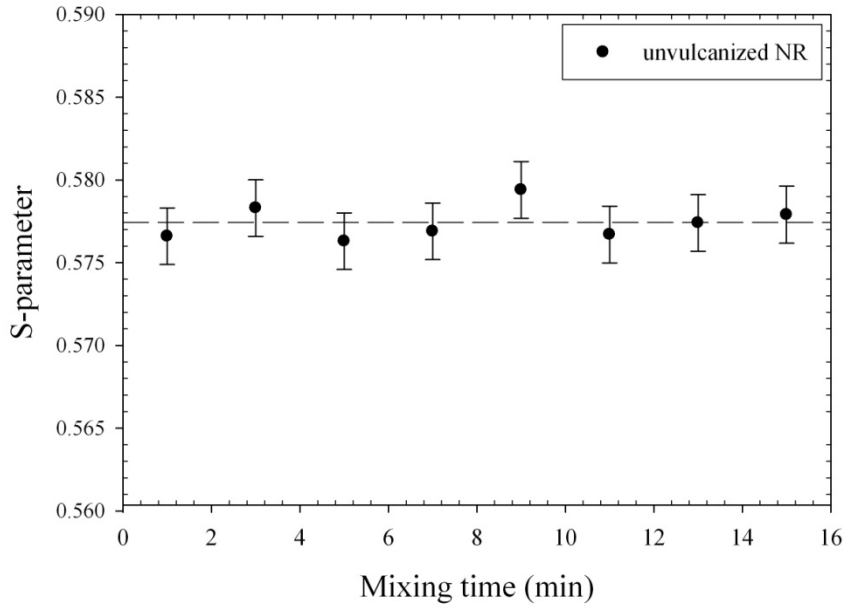

Figure 7.7 S-parameter vs. Mixing Time

VII.4 Effects of CB Parameters in rubber-CB composites

Carbon black which is a major compound in our composites plays a role of reinforcing rubber, as discussed earlier in the theory above. We specifically investigated two properties of CB by PAS which directly affect its reinforcing ability. These tests were necessary because sought to isolate the properties of the constituent compounds that had a direct effect on the Ps formation in the sample composites from those effects that resulted from structural changes in the sample. In this respect, we tried to understand the effect of CB morphology described by CDBP and surface area described by N_2SA. We used both PAL and DBS in these measurements and the samples used were vulcanized

NR and two vulcanized synthetic rubbers, D706 and Sn-SSBR each with 50 phr CB. Our investigations revealed that τ_3 is independent of N_2SA and CDBP as shown in figure 7.8 and figure 7.9 respectively, but it depends on the type of rubber used. Trend lines are drawn in these figures to guide the eyes. It is therefore reasonable at this point to state that τ_3 is a property of a given rubber. It should be noted that for a particular rubber used in this investigation, for example D706, different points have different CB grade of same phr.

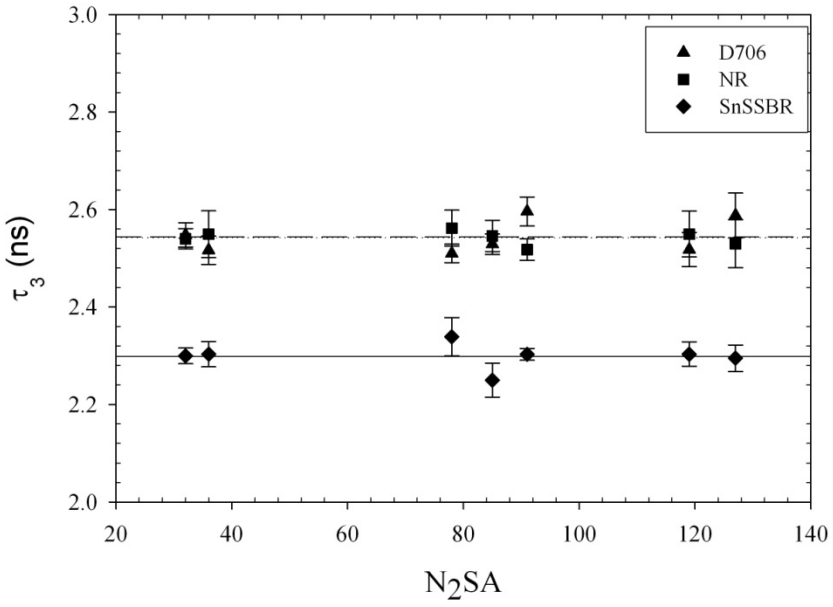

Figure 7.8 The o-Ps Lifetime, τ_3 vs. N_2SA.

Figure 7.10 shows that the ortho-positronium intensity I_3 depends on CB surface area. However from figure 7.11, our results suggest that CB structure has little affects on I_3. For example, in NR, in figure 7.11, the value of I_3 first increased then dropped with increasing CDBP. However, I_3 for D706 fluctuated with the increase in CDBP. The overall effect is a small drop in I_3 values.

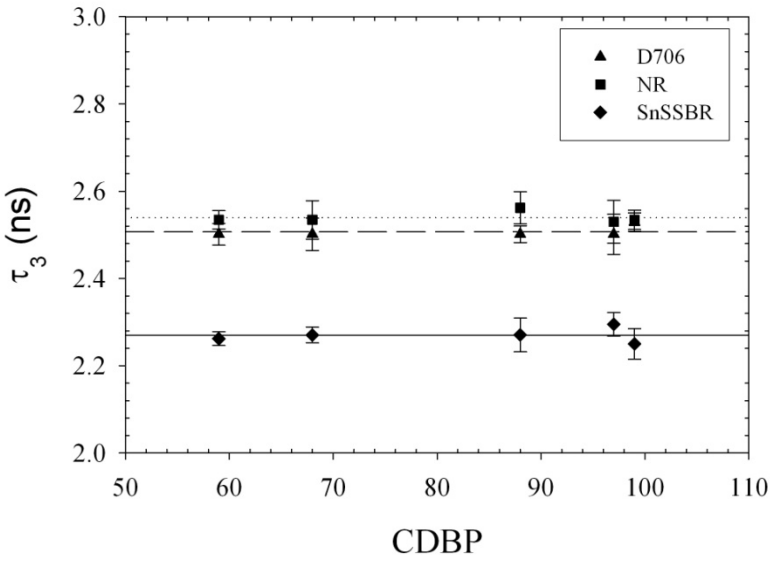

Figure 7.9 The o-Ps Lifetime, τ_3 vs. CDBP.

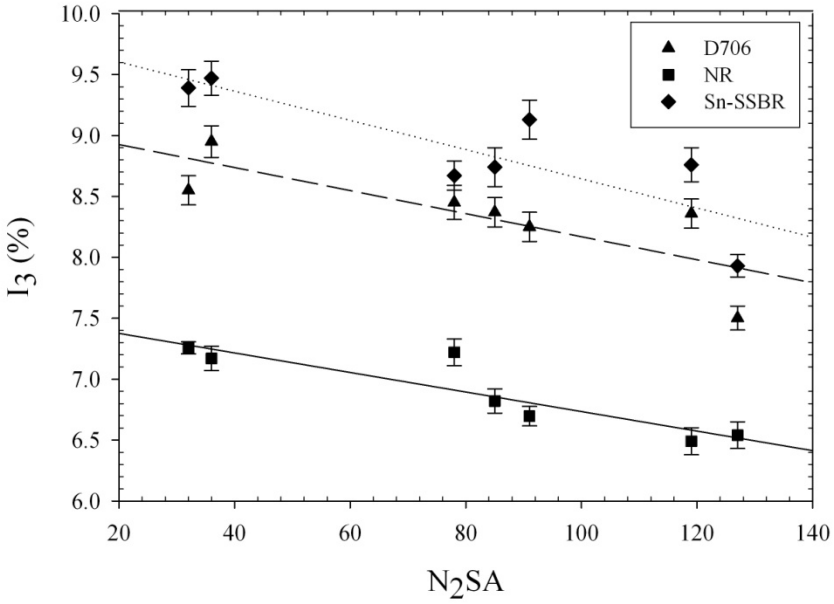

Figure 7.10 The o-Ps Intensity, I_3 vs. N_2SA.

Another observation is that I_3 depends on the type of polymer in question. S-parameter values for N_2SA, as seen in figure 7.12, behave the same way as I_3 values in figure 7.10. This suggests that S-parameter and I_3 are correlated and are sensitive to CB particles and to the extent of filler rubber interface interaction.

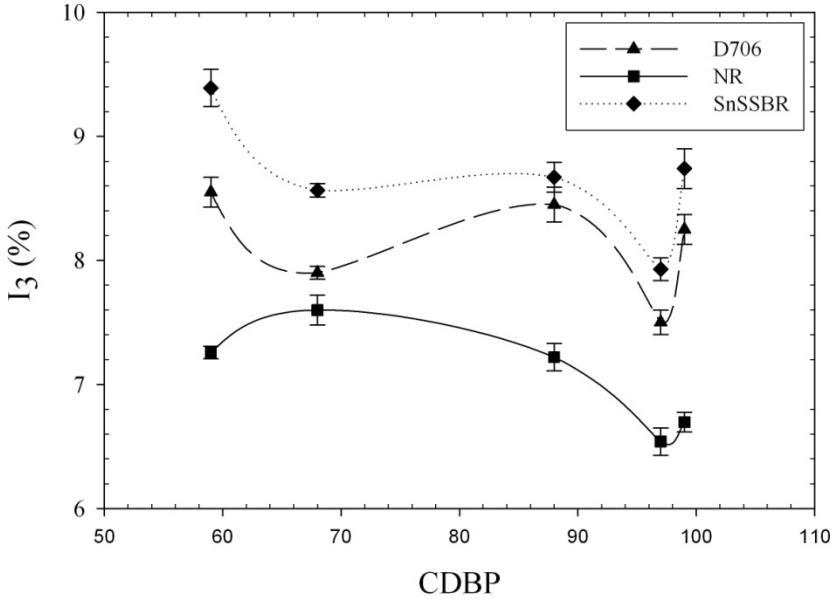

Figure 7.11 The o-Ps Intensity, I_3 vs. CDBP

S and I_3 are determined by positronium formed in the rubber. Increasing rubber-CB interaction decreases the positronium formation by providing an additional positron interaction mechanism, which competes with positronium formation in the rubber. S-parameter values show some decrease with increasing CDBP as can be seen in figure 7.13. This could be explained by whether the positron or the Ps is trapped in the bulk or near the CB surface where it is more constrained.

We should however point out that S-parameter and o-Ps intensity does not always correlate with one another.

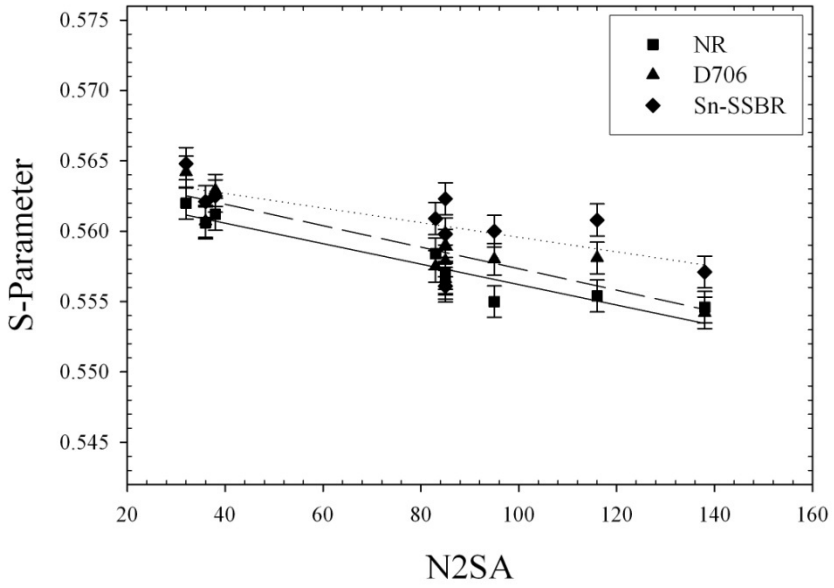

Figure 7.12 S-parameter vs. N_2SA

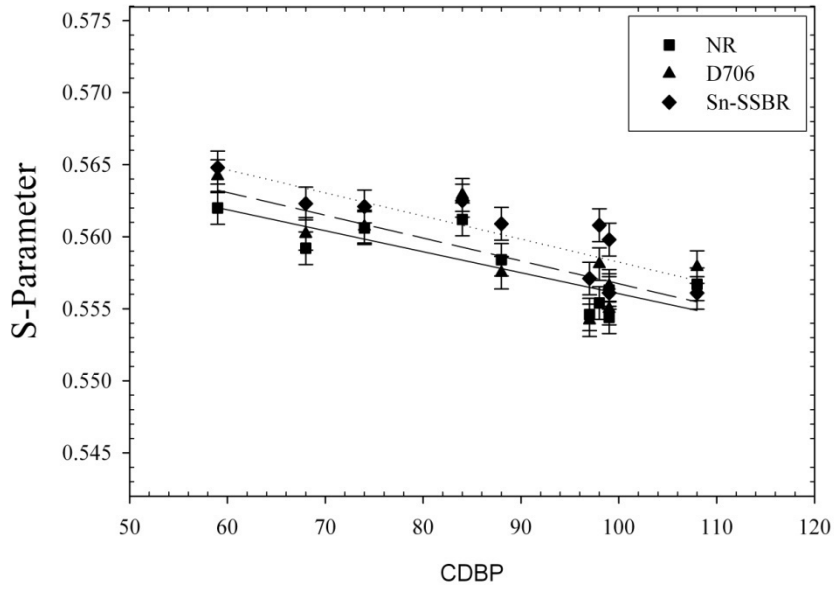

Figure 7.13 S-parameter vs. CDBP.

VII.5 Positronium formation in different complexes compared

At room temperature rubber has been found to be far above their glass transition temperature as compared to most general purpose polymers. This made us question whether treatingg rubber in the same category with other polymers was correct. Most polymers are generally hard at room temperature while rubber is soft and flexible at room temperature. Based on these observations, we carried out some investigations to compare the positronium response in rubbers, polymers and liquids. First we studied different liquids and rubbers, and then compared these results with those observed from the general polymers. It is important to remember that one of the goals of performing this research was to investigate the behaviour of rubber composites under different environmental conditions, hence a need for a proper model for data interpretation.

To study the liquids, the samples were made in small plastic sample cups with a kapton cover held on to the cup by a plastic sleeve. Na^{22} source was then sandwiched between two identical liquid samples before initiating the lifetime measurements. For rubbers, the source was sandwiched between two identical samples, and then lifetime measurement was initiated. For the liquids, the Ps atom is expected to dig a cavity or a bubble in them, thereby living longer within the bubble before annihilating. This has been attributed to its high zero-point kinetic energy [46] [55] [56]. For the rubbers, the Ps atom is expected to get confined within the free volume holes, living longer before finally annihilating by pick-off reaction.

Figure 7.14 shows S parameter versus o-Ps intensity for various liquids and rubbers used. It is interesting to note that S parameter for the rubbers looks like that observed for liquids. At room temperature, rubbers are far above their glass transition temperature (T_g

) and therefore behave more like liquids. This may also be explained as due to the formation of the bubble cavity in the rubber.

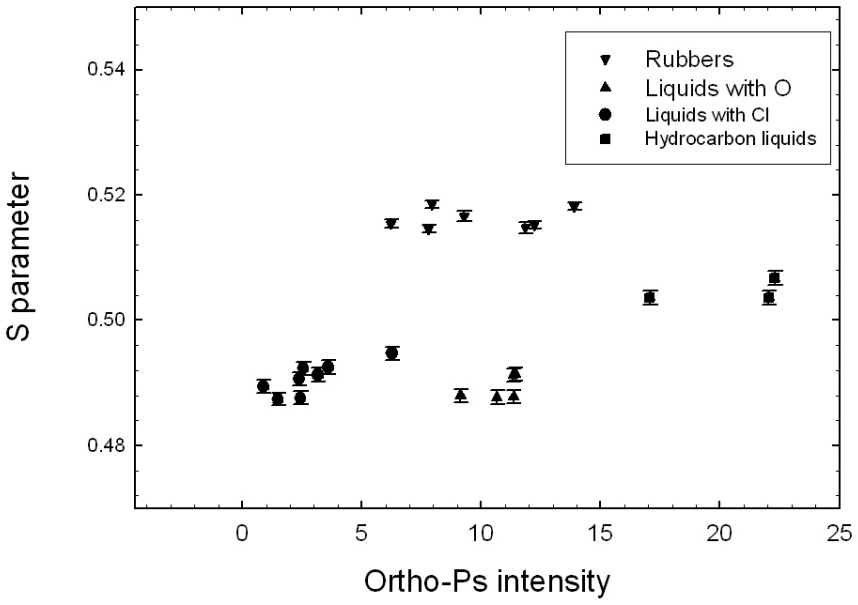

Figure 7.14 S-parameter vs. o-Ps Intensity for Various Liquids and Rubbers

We investigated the correlation between S parameter and o-Ps intensity for polymers with oxygen and nitrogen, rubbers and hydrocarbons to understand more about the nature and peculiarity of the rubbers. We were in the process of doing these investigations when a paper by Sato et al [56] appeared which ultimately corroborated our research.

S-parameter generally depends on the composition of the material since the presence of a higher atomic number will typically result in a higher probability of annihilation with core electrons and a decreased S-parameter. Polymers are generally hydrocarbons in nature so not much sensitivity of the S parameter to the composition is expected. S-parameter correlated well with o-Ps intensity for the polymers, as shown in figure 7.15.

The pure hydrocarbons tend to lie along the upper trend line, while oxygen bearing polymer samples lie on a trend curve below the hydrocarbons. The rubber samples however, seem to have a constant S parameter regardless of the o-Ps intensity.

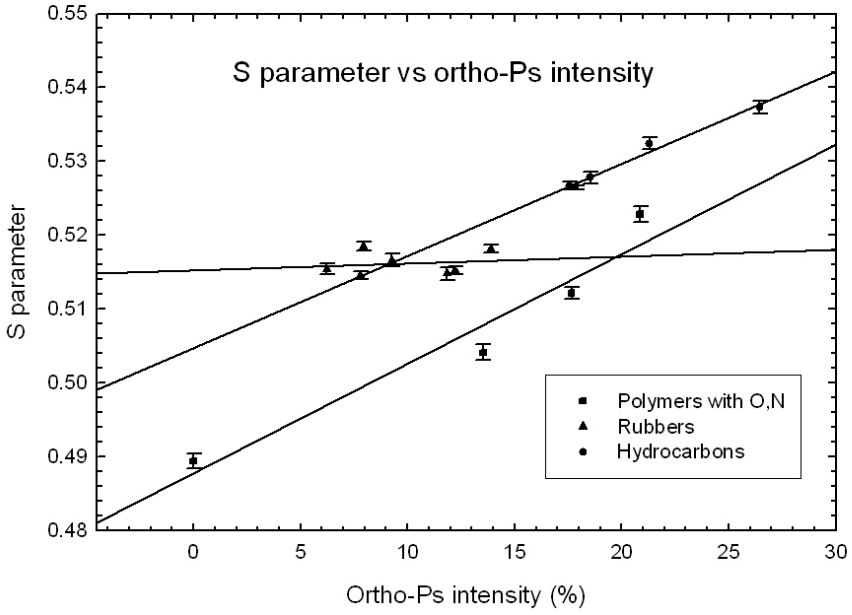

Figure 7.15 S-parameter vs. o-Ps Intensity (%) for Hydrocarbon Polymers with Oxygen and Nitrogen and Rubbers.

The change in S-parameter can only be understood if we think in terms of the positron direct and trapped annihilations compared with annihilations due to o-Ps formation. S-parameter is less for direct and trapped positron annihilation while larger for Ps annihilation, as seen by the slope of the trend line. Rubber, on the other hand, behaves like a liquid giving a relatively constant S parameter which has been attributed to the formation of the bubble cavity. These results are well aligned with the observations made by Sato et al and were presented at CAARI meeting in Fort Worth, TX in 2006. A paper about these results was submitted and has been accepted for publications in the Nuclear Instruments and Methods in Phys. Research journal [64].

VII.6 Determination of crosslink density in Natural Rubber

At this point we can naively say that rubbers are special type of polymer. Moreover, they have a cross-linked network structure and exhibit elastic behaviour, making them even more unique as compared to polymers. In that respect, we investigated the cross-link density in natural rubber and related this to the size of the bubble formed.

The samples we used in this study were both vulcanized and un-vulcanized natural rubber provided to us by Sid Richardson Carbon Black Company, Fort Worth TX USA. Table 7.1 summarizes the sample components.

COMPOUNDS	SAMPLE 1	SAMPLE 2	SAMPLE 3	SAMPLE 4
Natural Rubber	47.56	47.07	45.65	43.47
ZnO	2.38	2.35	2.28	2.17
Stearic Acid	1.43	1.41	1.37	1.3
Sulfur	1.19	2.35	5.71	10.87
MBTS	0.29	0.28	0.27	0.26

Table 7.1 Composition of Samples as mixed, before vulcanization, in grams.

To prepare the sample, rubber and vulcanizing additives were mixed in an internal mixer (Haake Rheocord 90) according to the ASTM D3191 standard recipe. For vulcanization, the samples material were transferred into a mold at 160^{o}C, which produced cylindrical samples with parallel surfaces of diameter 38 mm and thickness 15 mm. All vulcanized samples were heated for the same time regardless of the sulfur concentration.

VII.6.1 Swelling and cross-link density measurements

Toluene absorption has been used to study cross link density in polymers and rubber materials [34] [58] [61]. The extent at which the toluene molecules are imbibed in the sample material can be used to measure the flexibility of the molecular chains making up the network. The higher the toluene molecules imbibed in the sample, the more flexible the sample's chains are. This can be interpreted to mean that such a sample has less cross link density, whereas the lower the toluene content in the sample, the lesser the flexibility of the chains in the sample, meaning a higher cross link density. Several other methods such as Nuclear Magnetic Imaging (NMR), Differential Scanning Calorimetry (DSC), Fluorescence Polarization, and stress- strain measurements can also be used in studying the cross link density of the rubber sample. We preferred using toluene adsorption method in studying this cross link property of rubber to the other methods because of its cheap availability and easiness in handling. We also felt that toluene actually interact with the sample network completely as opposed to the other methods which give only average values of cross link densities based on indirect measurements.

The vulcanized sample for each sulfur concentration was cut and weighed on a balance capable of measuring to precision of 0.001g. The samples used were each approximately 16g. The samples were first weighed in air then soaked in toluene for different time intervals. The swollen specimens were blotted with filter paper and quickly transferred to the weighing pan. The process of soaking and weighing was continued until equilibrium swelling mass was attained. The sorption isotherms showing mass-time curves were plotted in figure 7.16 below. At the equilibrium mass values; the value of the

network chain density was calculated for each sulfur concentration in the network via the modified Flory-Rehner equation [34] [61]:

$$v = \frac{-[\ln(1-V_r)+V_r+\chi V_r^2]}{V_o(V_r^{\frac{1}{3}}-\frac{2V_r}{f_c})} \tag{20}$$

where v is the network chain density per unit volume of rubber (mol/cm^3), f_c is the functionality of crosslink, χ is the interaction parameter of the polymer solvent, V_o is the solvent molar volume (cm^3/mol) and V_r is the volume fraction of the sample at equilibrium of swelling defined by:

$$V_r = \frac{1}{1+Q} \tag{21}$$

where Q is the volume of imbibed solvent per unit volume of polymer; that is

$$Q = \left(\frac{W_s}{W_n}\right)\frac{\rho_r}{\rho_s} \tag{22}$$

W_s is the weight of the solvent in the network and W_n is the weight of the network; ρ_s is the solvent density (g/cm^3); ρ_r is the rubber density and was founded by dividing the mass of a known rubber sample by its volume. The constants used in this study are [34], f_c=4, ρ_s=0.87 g/cm^3, V_o=106.29 cm^3/mol, χ=0.42. The cross-link density as a function of sulfur concentration in the samples was then plotted in figure 7.17. As expected, the cross-link density increased with sulfur concentration.

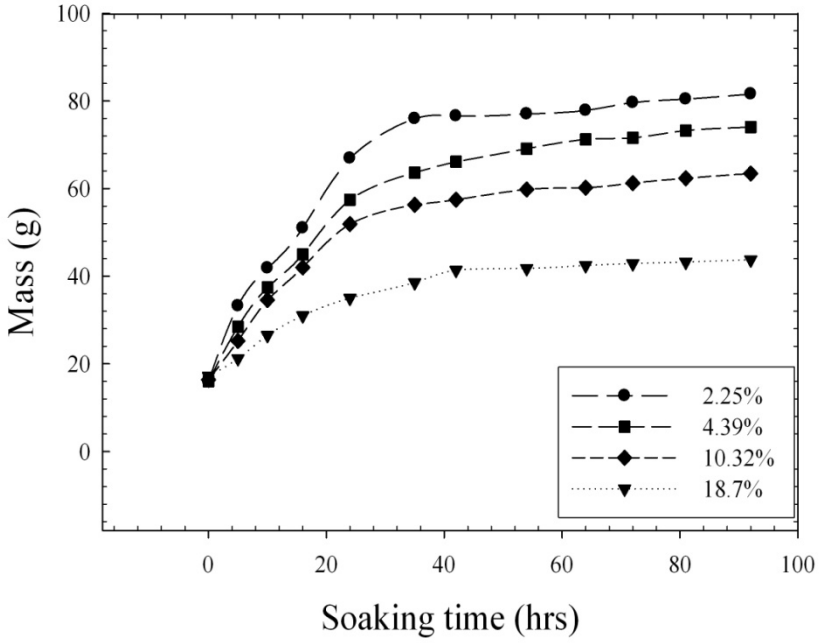

Figure 7.16 The Mass of the Rubber-Toluene Network vs. Soaking Time

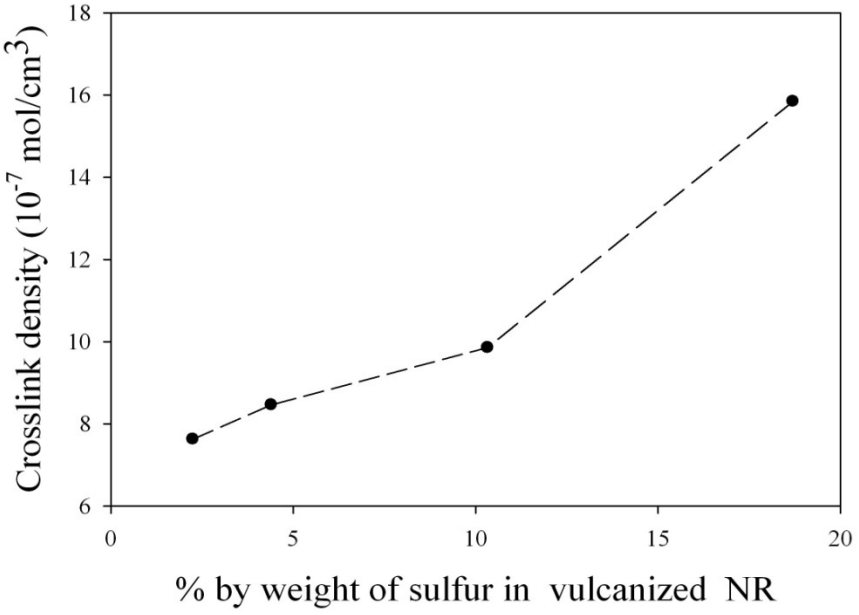

Figure 7.17 Cross-link density vs. % of Sulfur by Weight in NR

The diffusion coefficient of toluene in natural rubber was also estimated from a half-life relation [58] based on figure 7.16 above, with 2.25% sulfur concentration in NR

corresponding to the normal sulfur concentration used in the common vulcanized natural rubber samples for industrial applications,

$$D = \frac{0.0492L^2}{t_{\frac{1}{2}}} \tag{23}$$

where L is the thickness of the dry sample in centimetres and $t_{\frac{1}{2}}$ is the time in seconds for one-half the equilibrium weight gain. The quantity obtained, D, is the natural rubber mass-fixed diffusion coefficient and the value we obtained was $2.8\text{x}10^{-08}$ cm^2/s and was found to be of the same order of magnitude ($1.8\text{x}10^{-07}$ cm^2/s) as was found by the group in reference [58].

The results in this section were presented at ICPA conference in 2006 and submitted for publications in the Radiation Physics and Chemistry journal [65].

VII.6.2 PAL Measurements on vulcanized and un-vulcanized NR samples

The o-Ps lifetimes and intensities for both vulcanized and un-vulcanized NR samples were plotted in figure 7.18 and figure 7.19 respectively. Both τ_3 and I_3 decreased with sulfur concentration in the vulcanized and un-vulcanized NR samples. However, the decrease for the vulcanized sample was more than for the un-vulcanized one. For the un-vulcanized sample, the sulfur inhibited Ps formation; hence the decrease in I_3 with sulfur weight %. For the un-vulcanized sample, there was a slight decrease in τ_3 from the sample with zero sulfur and then τ_3 remained relatively constant with increase in weight

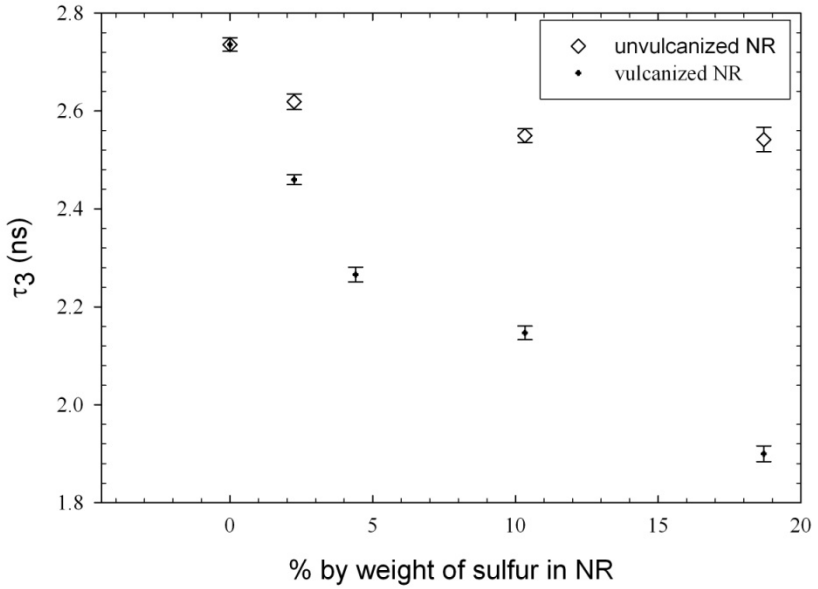

Figure 7.18 The o-Ps Lifetime vs. % of Sulfur by Weight in NR.

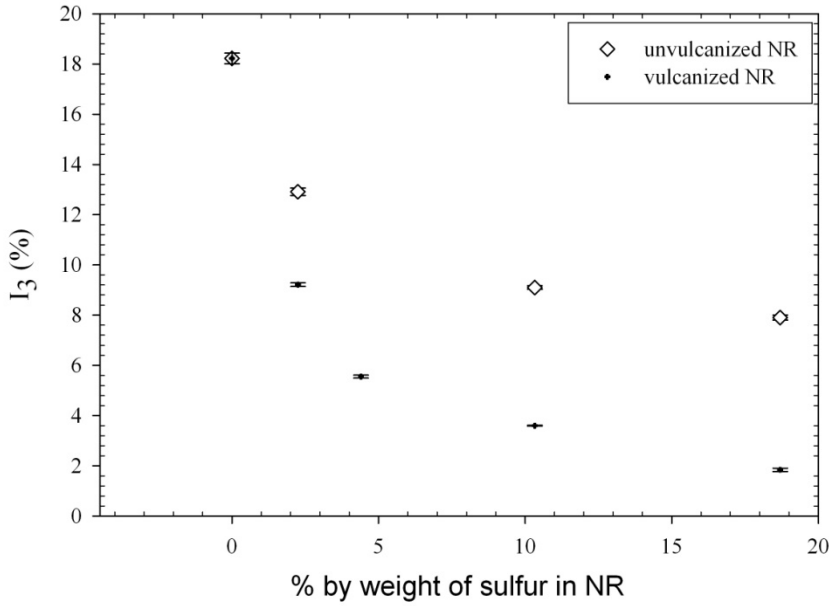

Figure 7.19 The o-Ps Intensity vs. the % of Sulfur by Weight in NR.

percent of sulfur. It is believed that some chemical reaction can occur during the mixing and heating of the rubber with sulfur and other additives. As a result, some cross-links are

formed even without formal vulcanization which leads to a small decrease in τ_3 as seen in figure 7.18.

When the sample is vulcanized, sulfur melts and mixes well with the polymer network. Sulfur molecules form cross-link bonds with the polymer chains and thereby reinforce the structure. With vulcanization, and the increase of cross-linking, both τ_3 and I_3 decreased significantly more than the un-vulcanized sample, as shown in figure 7.18 and 7.19 respectively. Recall that the increase in weight % of sulfur can be interpreted as an increase in cross link density (fig. 7.17). The significant decrease in τ_3 with weight % of sulfur or cross link density can be understood as being due to the decrease in mobility of the polymer chains caused by the increase in cross links. The Ps is not able to make for itself as large a bubble as it can at high cross-link densities.

For the vulcanized sample, part of the decrease in I_3 seen in figure 7.19 is due to Ps inhibition by the sulfur as seen for the un-vulcanized samples. The further decrease in I_3 or free volume can be understood as the result of cross linking. As cross link density increases there is reduced mobility of the polymer chains and thus a reduction in the size of the bubble and in I_3.

From the Tao-Eldrup model, we calculated the free volume and plotted the results as shown in figure 7.20. As expected, and since the free volume is a linear function of o-Ps lifetime, free volume decreased with increase in percent weight of sulfur. The decrease also depended on whether the sample was vulcanized or un-vulcanized. From the free volume and the o-Ps intensities, we calculated the fractional free volume in the sample and plotted, as in figure 7.21 below. Free volume also decreased with increasing percent weight of sulfur in the sample.

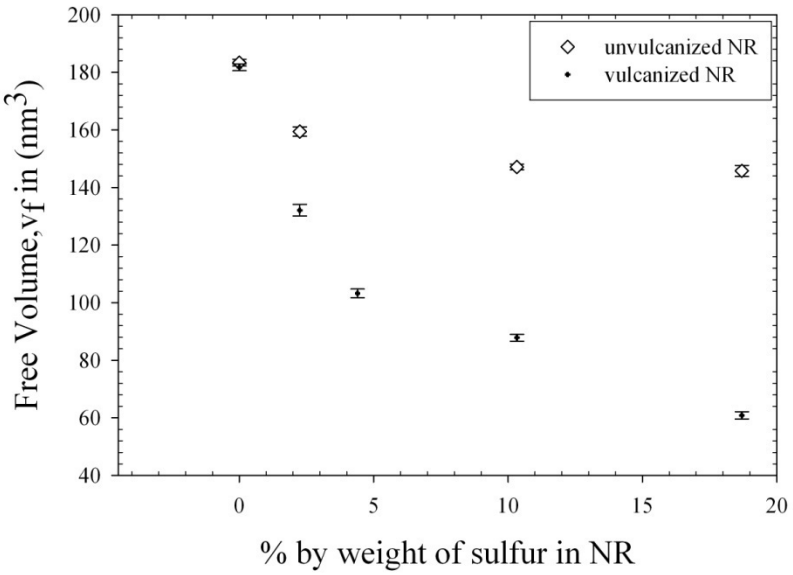

Figure 7.20 The Free Volume vs. % by Weight of Sulfur in NR.

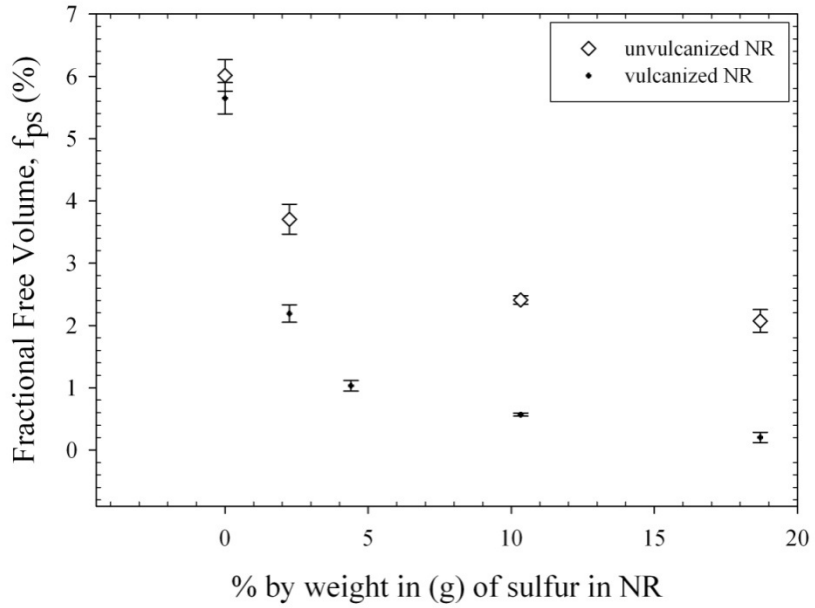

Figure 7.21 The Fractional Free Volume vs. % by Weight of Sulfur in NR.

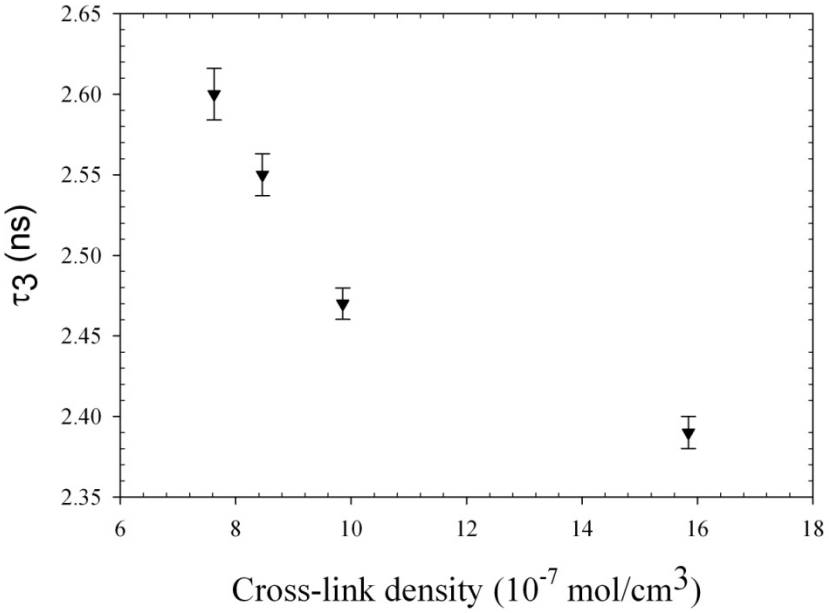

Figure 7.22 The o-Ps Lifetime vs. the Cross-link Density

Finally we calculated the cross-link densities and plotted as a function of o-Ps lifetime, o-Ps intensity, free volume and fractional free volume as shown in figure 7.22

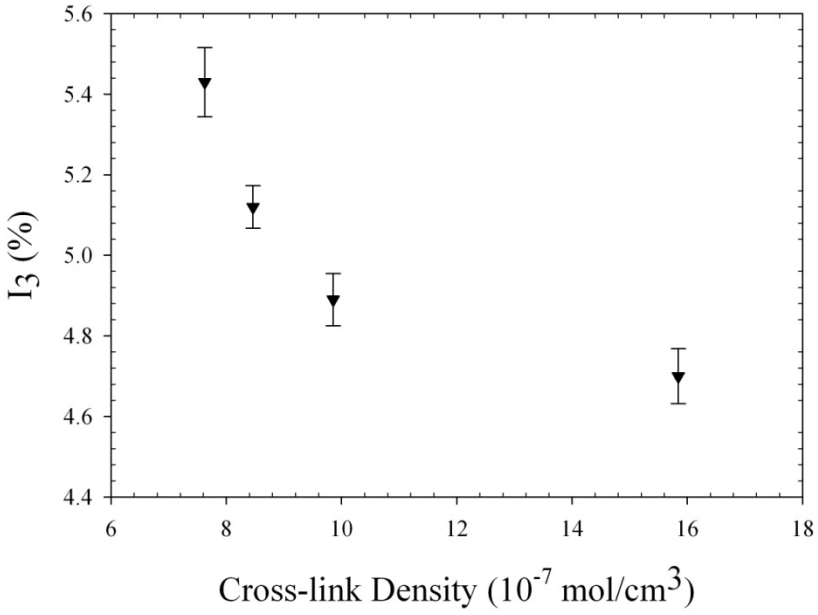

Figure 7.23 The o-Ps intensity vs. Cross-link Density.

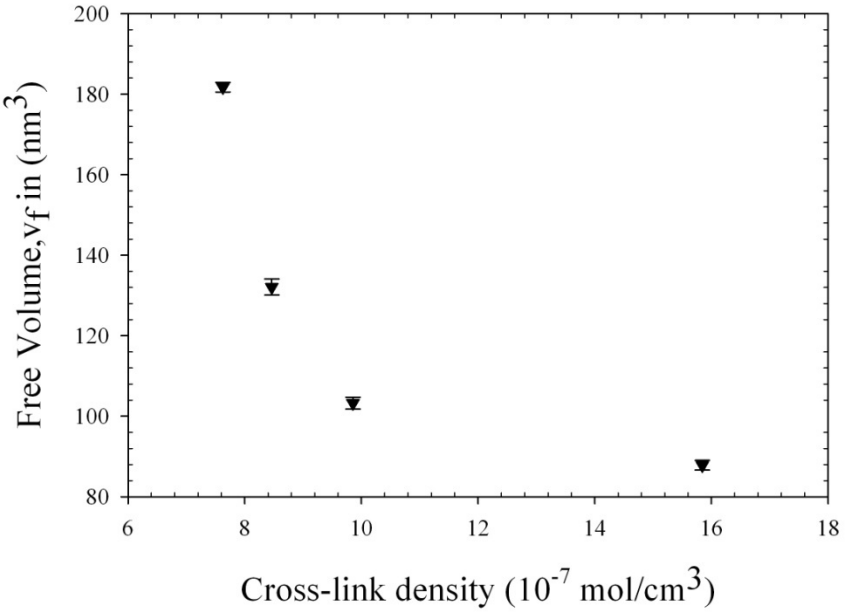

Figure 7.24 The Free Volume vs. Cross-link Density

through figure 7.25. As can be observed, there is a correlation between the crosslink density and the per cent weight of sulfur in the samples.

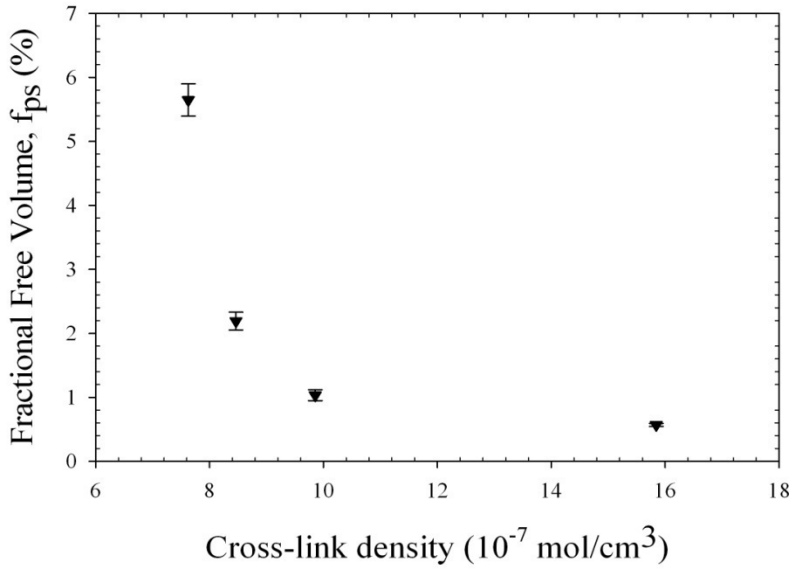

Figure 7.25 The Fractional Free Volume vs. the Cross-link Density.

VII.6.3 Conclusions

Sulfur molecules cross-link polymer chains thereby reducing the polymer chain mobility. The annihilation of the Ps atom in the bubble dominates that in the pre-existing free volume holes. Increase in cross-link density hence limits the size of the bubble which is seen as a decrease in the o-Ps lifetime. Both the equilibrium swelling and PAL measurements agree well and suggest that the amount of cross-links in the polymer network controls the structural behaviour of the polymer.

The results from this section were presented at the ICPA conference in 2006 and a paper submitted for publication in Radiation Physics and Chemistry journal [65].

VII.7 Aging of Natural Rubber and Synthetic Rubber Carbon Black Composites

VII.7.1 Curing Process

After knowing and understanding our sample network well, we finally embarked on investigating by PAL how the sample network is affected under different conditions. Our first test was to investigate the natural rubber curing process in the lab based on the normal standard recipes and conditions**.** In this investigation, we used NR samples with 50 phr CB. The sample material was heated at 160 ^{o}C in an oven capable of measuring temperature to an accuracy of ±1 ^{o}C. Heating was done at an interval of 3 minutes, then the sample was cooled immediately in ice water before initiating lifetime measurement. The measurements were initiated within the first 15 minutes of cooling. Cumulatively, each sample was heated for about 20 minutes

Figure 7.26 shows the behavior of the longest lifetime, τ_3, as a function of curing time for both NR and D706 rubber samples. Lines are drawn to guide the eyes. NR rubber

underwent a cycle as can be seen in figure 7.26. The first stage shows a decrease in τ_3 indicating a decrease in the average size of the free volume hole. This we ascribed to the cross-links formation between NR and sulfur. Then τ_3 reached a minimum which suggests a maximum cross-link density. Then in the last stage, τ_3 increased which suggests that the cross-links broke upon further curing resulting in an increase in the average free volume hole. This process is commonly known as *rubber reversion* and is a thermally driven process whereby a vulcanized natural rubber reverts back to the un-vulcanized gum state as a result of heat [11]. On the other hand, within the same time range and temperature, τ_3 for D706 slowly decreased without showing any cyclic behavior. This suggests that the cross-links formed between D706 chains and sulfur atoms are stable and stronger under heat as compared with those of NR.

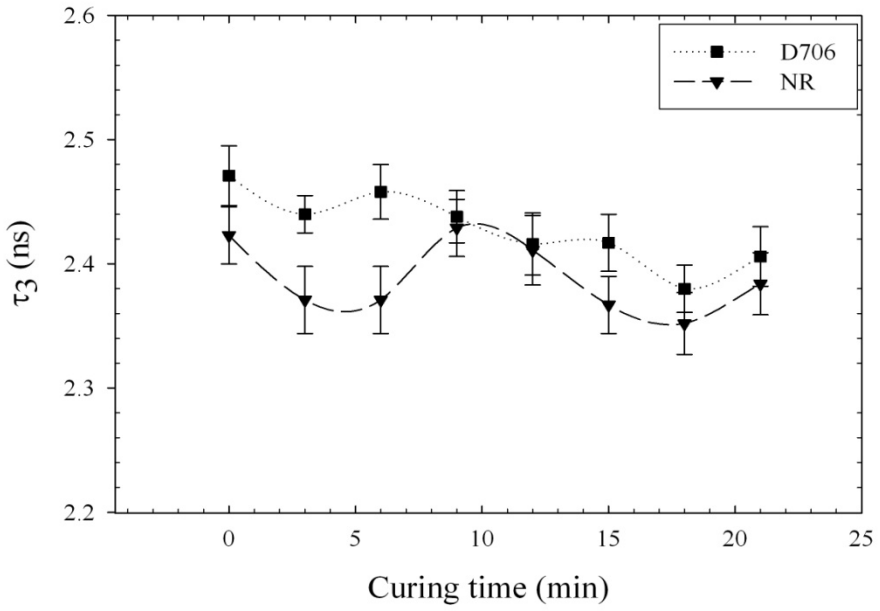

Figure 7.26 The o-Ps Lifetime vs. Curing Time

Figure 7.27 shows the free volume behavior as a function of curing time. It correlates with the o-Ps lifetime whereby the free volume for NR shows reversion while that for D706 decreases gradually. Figure 7.28 shows the longest o-Ps, I_3 for both NR and D706 versus curing time. I_3 for NR decreases then passes through a minimum, just like its o-Ps lifetime component. It is expected that when the average free volume hole size increases, the number of free volume holes also increase. This further supports the concept of the reversion of natural rubber. However, I_3 for D706 does not change with curing time, suggesting the stability of its cross-links. By calculating the radius of the free volume based on the o-Ps lifetime τ_3 from eq. 38 in the appendix, we can

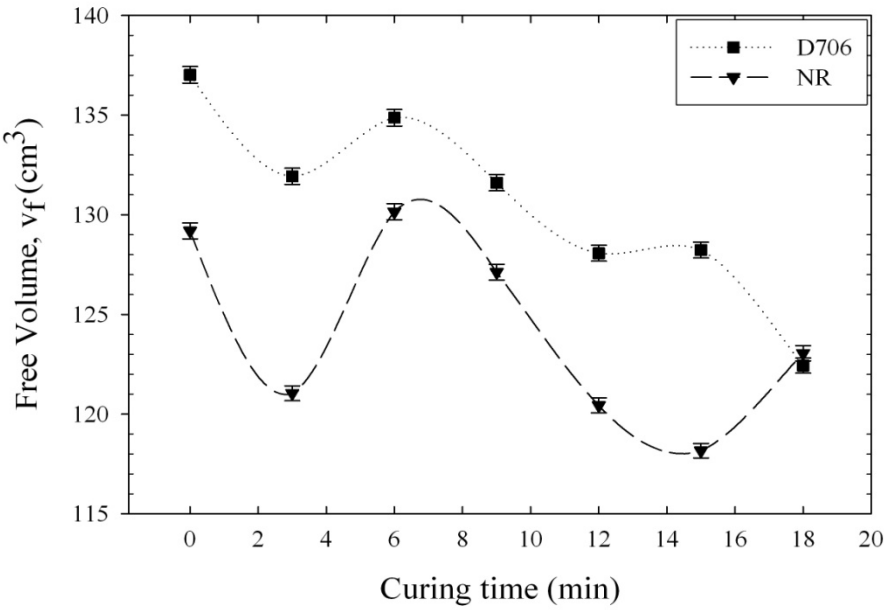

Figure 7.27 The Free Volume vs. Curing Time

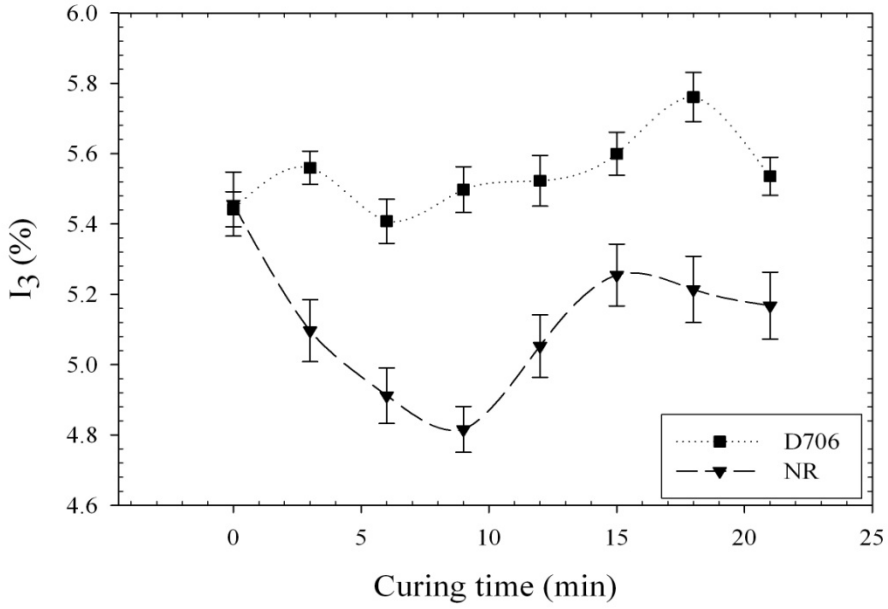

Figure 7.28 The o-Ps Intensity vs. Curing Time

determine the free volume using eq.39. Then, using eq.10, the fractional free volume f_v could be calculated. As seen in figure 7.29, f_v for D706 gradually decreased with curing time while that of NR rapidly decreased to a minimum and then started fluctuating with curing time which suggests the instability of natural rubber with longer curing time.

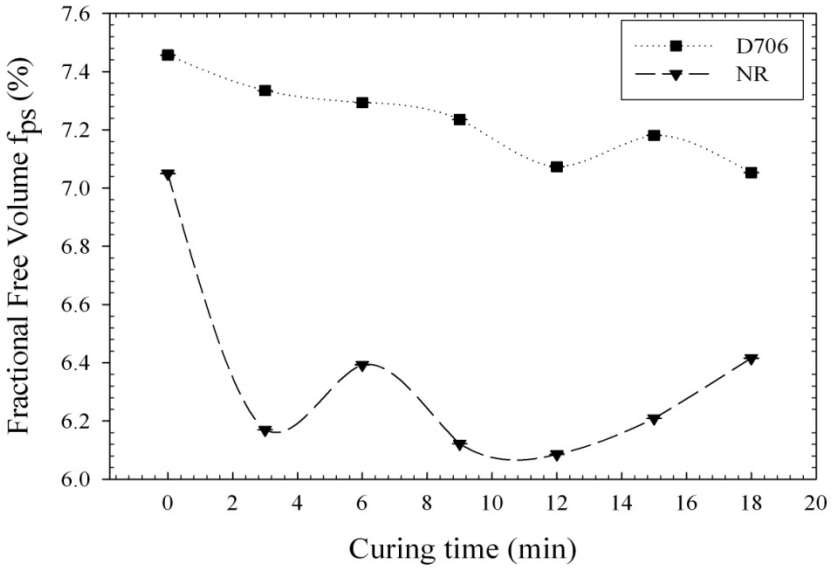

Figure 7.29 The Fractional Free Volume vs. Curing Time.

The results in this section were presented an ICPA conference in 2006 and a paper was submitted for publication in the Radiation Physics and chemistry journal [66].

VII.7.2 Aging Measurements

We sought to understand the relaxation behavior of NR-50phr of N330 CB composites by the use of both PAL and DBS. We investigated the relaxation process for uncured and cured samples at room temperature and at elevated temperatures both in air also in a vacuum. The free volume behavior as a function of time during isothermal relaxation was compared for the different heat treatments.

VII.7.2.1 Low Temperature Studies

Two cured and uncured samples were put in an incubator capable of measuring temperature to about $100\,°C$ to an accuracy of $\pm 1°C$. The samples were heated at $60\,°C$ for 12 hrs and allowed to cool down in a desiccator. After which lifetime and DBS measurements were performed and resulting spectra analyzed. The other two cured and uncured samples were left in the dessicator at room temperature and lifetime and DBS measurements carried out after an interval of one to two days.

VII.7.2.1.1 Isothermal Aging at Room Temperature

Vulcanized and un-vulcanized samples were aged at room temperature for a period of two months while measurements were periodically taken measurements to monitor the free volume relaxation behavior**.** To minimize the effect of oxidation, the samples were left to age in a desiccator connected to a vacuum pump. The data collection time was approximately 60 minutes at each time period corresponding to 10^6 counts.

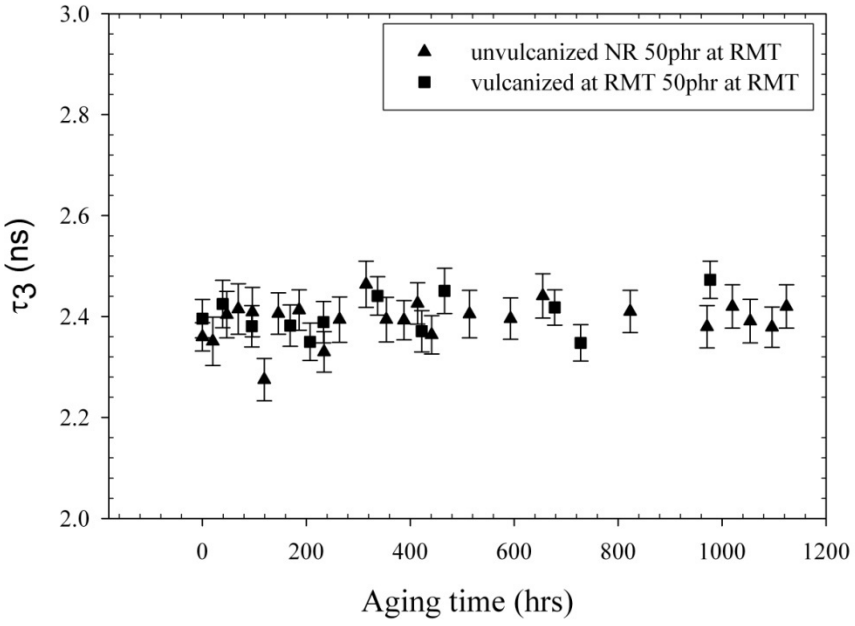

Figure 7.30 The o-Ps Lifetime, τ_3 vs. Aging Time for Un-vulcanized and Vulcanized Natural Rubber –CB samples at Room temperature

Figure 7.30 shows that τ_3 for both un-vulcanized and vulcanized samples remained unchanged with time. I_3 also remained constant with time as shown in figure 7.31. In comparison, figure 7.31 shows that the I_3 values for un-vulcanized samples were higher than those of vulcanized samples. This implied that un-vulcanized samples had more free volume holes than vulcanized ones.

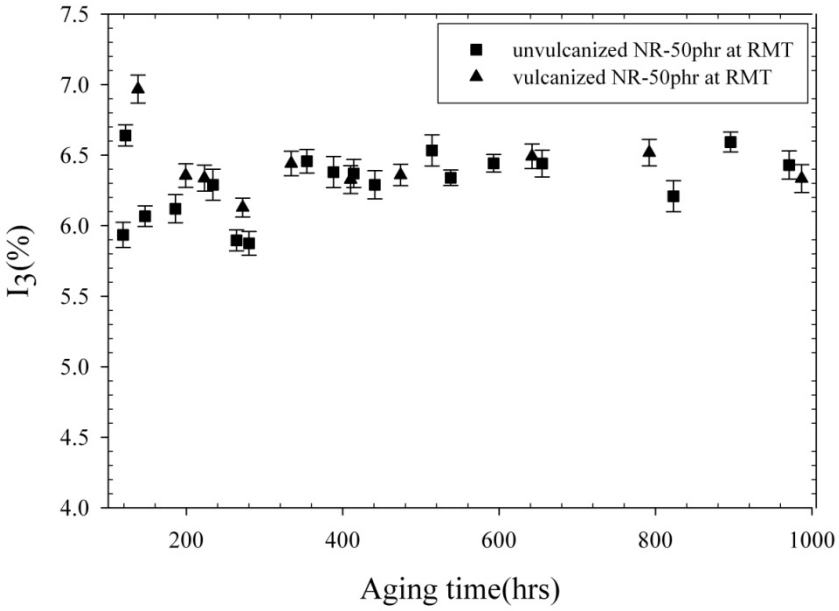

Figure 7.31 The o-Ps Intensity, I_3 vs. Aging Time for Un-vulcanized and Vulcanized Natural Rubber- CB samples at Room temperature.

VII.7.2.1.2 Samples heated at 60° C then cooled to room temperature

Vulcanized and un-vulcanized samples were annealed at 60° C for a period of 12 hrs and allowed to cool to room temperature for another 12 hrs. Then the lifetime and DBS measurements were initiated. We assumed that after cooling for 12 hrs, the samples had attained their equilibrium state. The same samples were heated, cooled and measured repeatedly for about two months. Results showed both τ_3 and I_3 for vulcanized samples at this temperature range remained unchanged as shown in figure 7.32 and figure 7.33 respectively. The DBS result was also plotted, as shown in figure 7.34, and supported the idea that I_3 for vulcanized sample remained constant for both treatments.

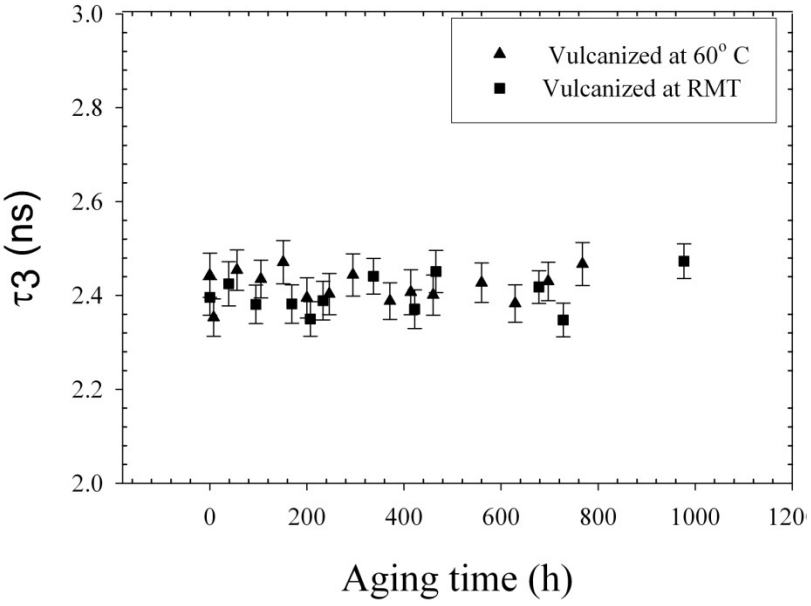

Figure 7.32 The o-Ps Lifetime, τ_3 vs. Aging Time for Vulcanized Natural Rubber 50phr at 60° C and at Room Temperature.

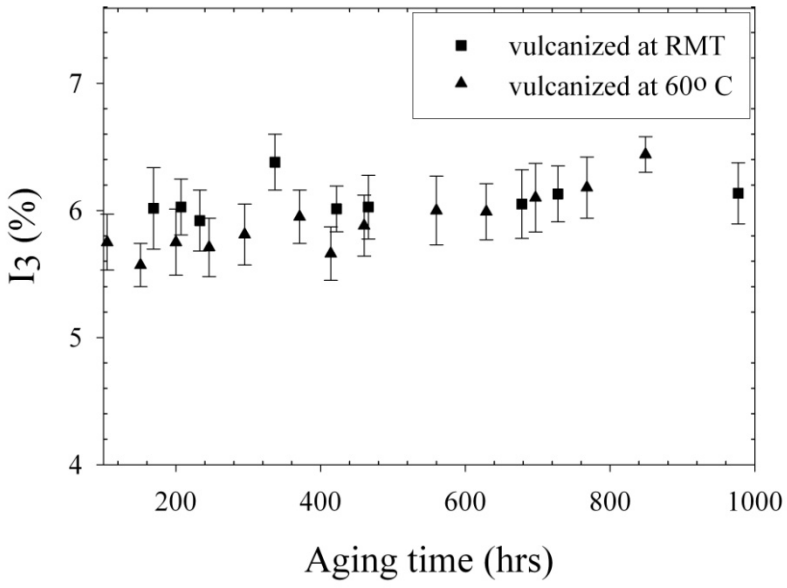

Figure 7.33 The o-Ps Intensity, I_3 vs. Aging Time for Vulcanized Natural Rubber, 50phr at 60° C and at Room Temperature.

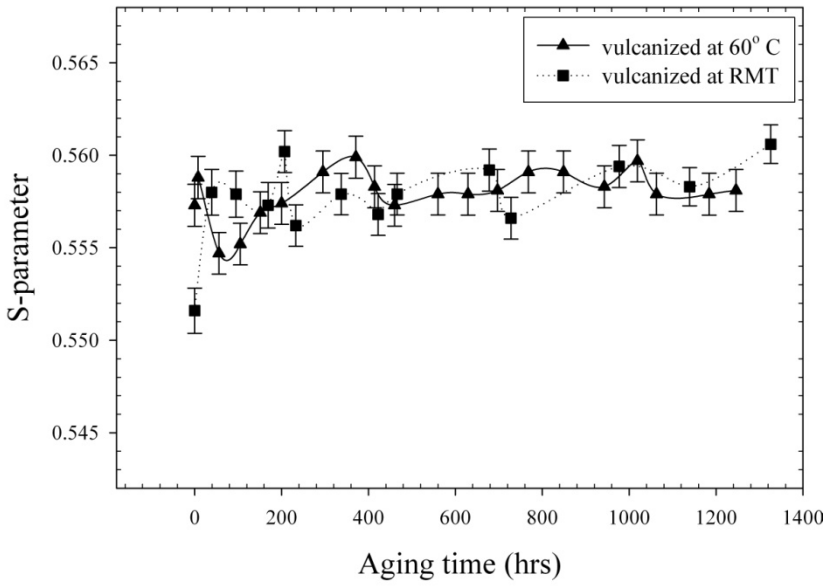

Figure 7.34 S-parameter vs. Aging Time for Vulcanized Sample, 50phr-NR at 60° C and at Room Temperature.

However, both τ_3 and I_3 for un-vulcanized samples showed lower values for the heated sample as compared to the un-heated one as shown in figure 7.35 and figure 7.36. In fact I_3 values decreased gradually to a near constant value. These showed that both the free volume size characteristic of the positronium lifetime and free volume holes were decreased as a result of this heat treatment for the un-vulcanized samples.

Decrease in I_3 generally suggests diminishing free volume hole distributions. As earlier indicated, free volume holes exist in the polymer chains. Therefore, when their distributions decreased, we expected the polymer chains to assume some compactness. Figure 7.36 illustrates this behavior and we interpreted this as *crystallization* of natural rubber. We should also point out that other reactions such as oxidation of the rubber chains which increase with heat could also be a possible cause for the decrease in o-Ps intensity. This oxidation leads to inhibition of o-Ps formation and quenching of o-Ps lifetime.

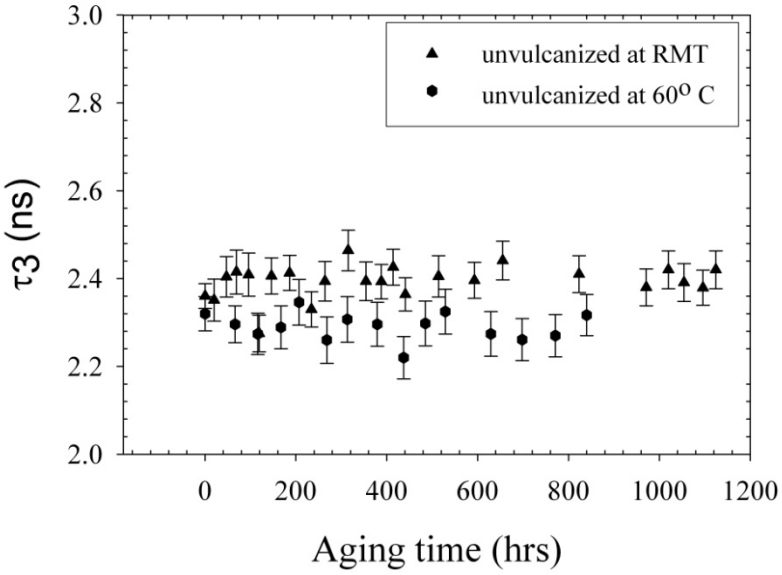

Figure 7.35 The o-Ps lifetime, τ_3 vs. Aging Time for Un-vulcanized Natural Rubber 50phr at 60° C and at Room Temperature.

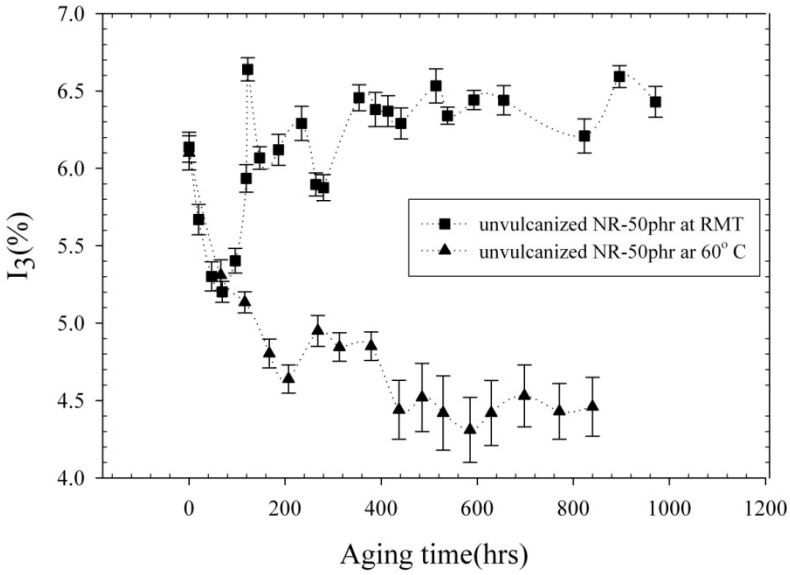

Figure 7.36 The o-Ps intensity, I_3 vs. Aging Time for Un-vulcanized Natural Rubber, 50phr at 60° C and at Room Temperature.

We made some comparison between un-vulcanized results and vulcanized ones as shown in figure 7.37 through 7.39 below. We found that at 60° C, only the un-vulcanized samples showed any significant changes in their network.

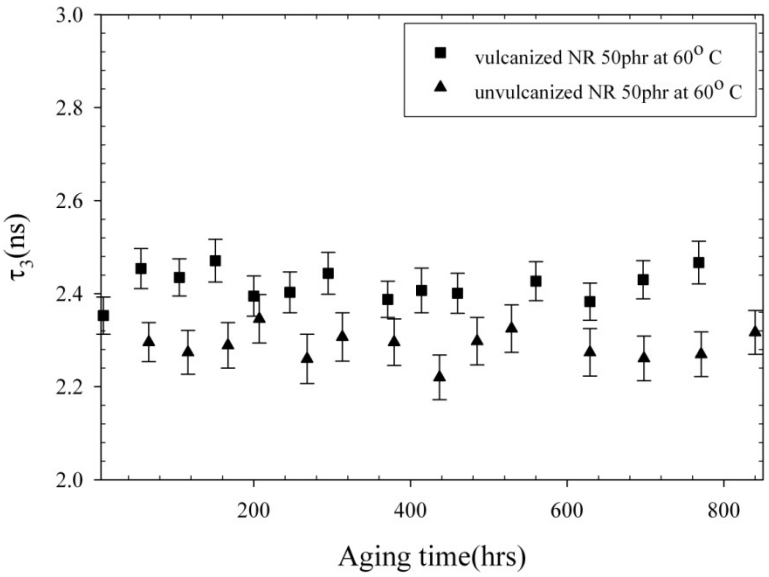

Figure 7.37 The o-Ps Lifetime vs. Aging Time for both Vulcanized and Un-vulcanized at 60° C.

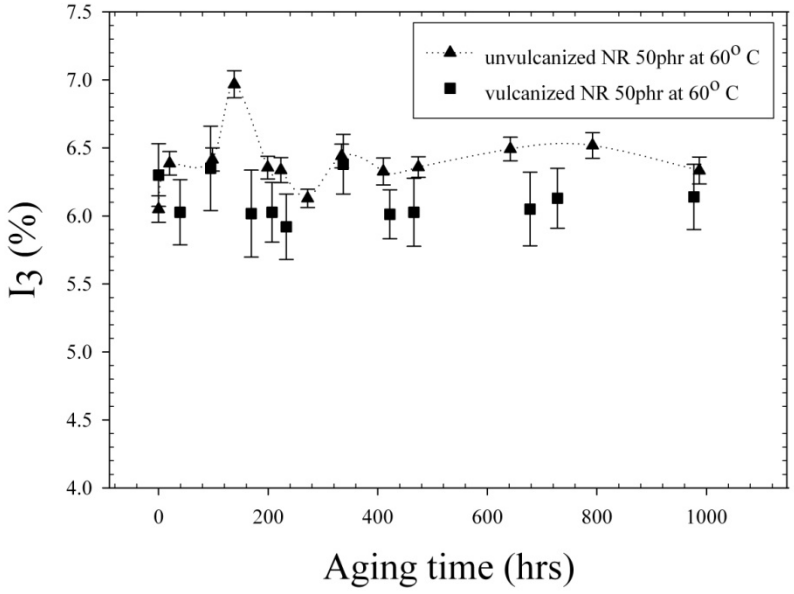

Figure 7.38 The o-Ps Intensity vs. Aging Time for Vulcanized and Un-vulcanized Samples at 60° C

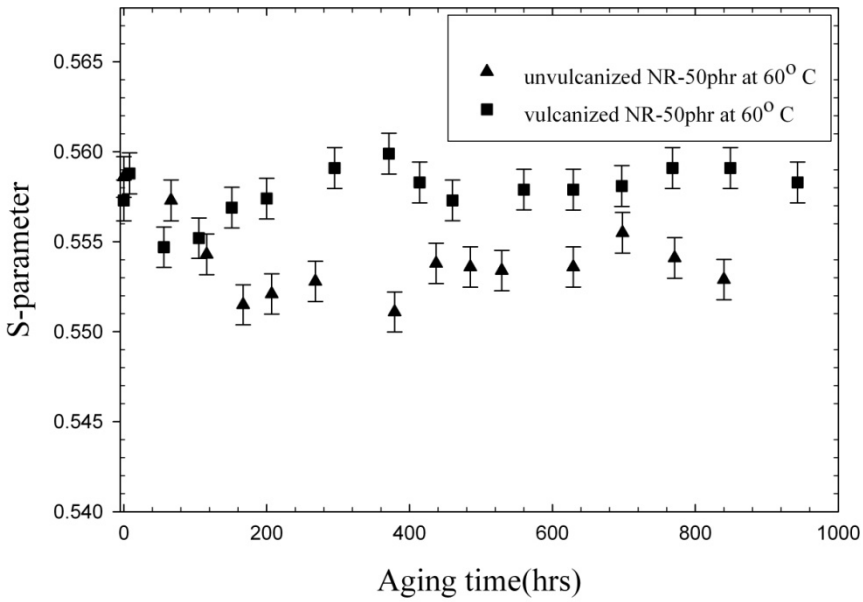

Figure 7.39 S-parameter vs. Aging Time for Vulcanized and Un-vulcanized Samples at 60° C.

VII.7.2.1.3 Reversibility Test

One un-vulcanized NR 50phr sample was left to age at room temperature while the lifetime spectra were measured periodically. Another similar one was heat treated at 60° C for 12 hrs and allowed to cool for a further 12 hrs before taking lifetime measurements. This process was repeated for these samples for two months. Then the samples were reversed so that the first one was now heat treated while the second one was left at room temperature. The results were analyzed and plotted as shown in figure 7.40.

I_3 for sample A decreased gradually when heat-treated for the first 900 hrs .During this period, I_3 for sample B kept at room temperature remained constant. Upon reversing this treatment, by which sample A was now left at room temperature and sample B was heated, I_3 for sample A increased while it decreased for sample B. Given that the two samples were same both chemically and physically before the start of the experiment, we

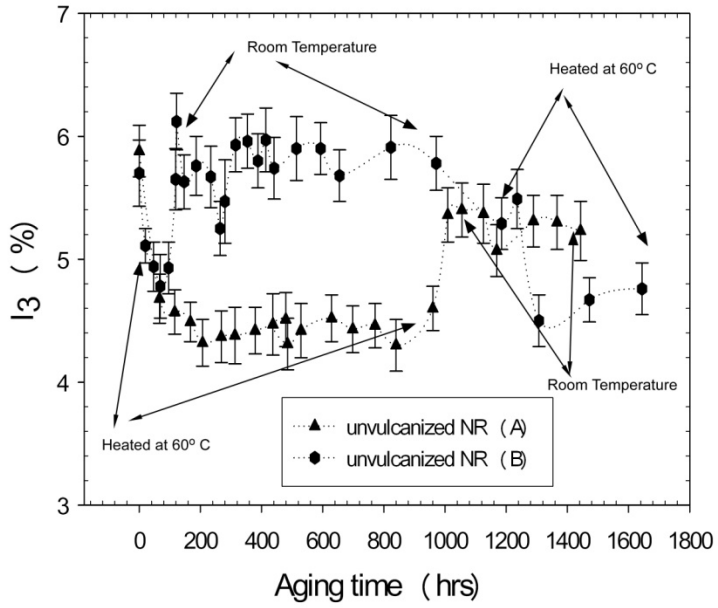

Figure 7.40 The o-Ps Intensity, I_3 vs. Aging Time for Un-vulcanized Sample A and sample B (both 50phr CB).

expected I_3 for sample A upon increasing, to be completely at same level with that of sample B. However, this was not the case as can be seen in the figure 7.40. I_3 values for sample A increased and stabilized at a little bit lower values compared to those of sample B. This suggested that some permanent change occurred during heating sample A; an aspect of chemical aging mechanism. This result also demonstrated reversibility of un-vulcanized natural rubber during physical aging. The permanent change could mean that the un-reacted sulfur formed more cross-links with sulfur thereby decreasing the number of free volume holes in the sample.

VII.7.2.2 High Temperature Studies

We tried to investigate the response of the free volume at elevated temperature for Natural Rubber-CB N330, 50phr. We did this by heating the samples at 160^o C over a

long period of time while periodically taking measurements. It should be noted that all our lifetime measurements were initiated after cooling the samples to room temperature. Cooling not only preserved the thermal history of samples, but also made it easier to handle the samples and avoid any fluctuations in PAL data points. We used both synthetic rubber, D706, and natural rubber with 50phr carbon black. The results were analyzed and reported as shown below. As can be observed from figure 7.41 and figure 7.42 below, the o-Ps lifetime and intensity for NR underwent some cyclic behavior during the first 160 hrs of heating, and then finally stabilized on continued heating. This behavior of NR is unique and was also observed during curing. We attributed this to reversion of chains leading to a decrease in both o-Ps lifetime and intensity above 160 hrs of heating. On the other hand, both the o-Ps lifetime and intensity for D706 decreased a little bit then stabilized.

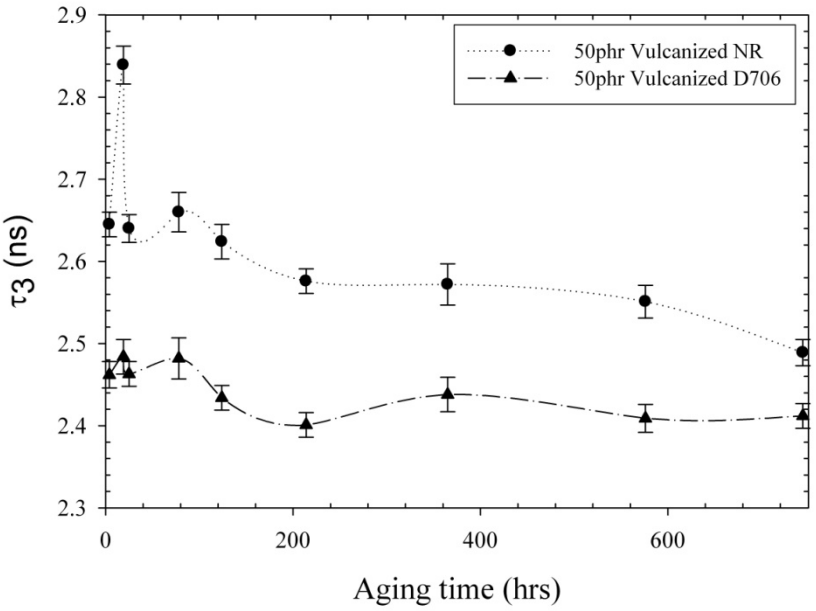

Figure 7.41 The o-Ps Lifetime vs. Aging Time.

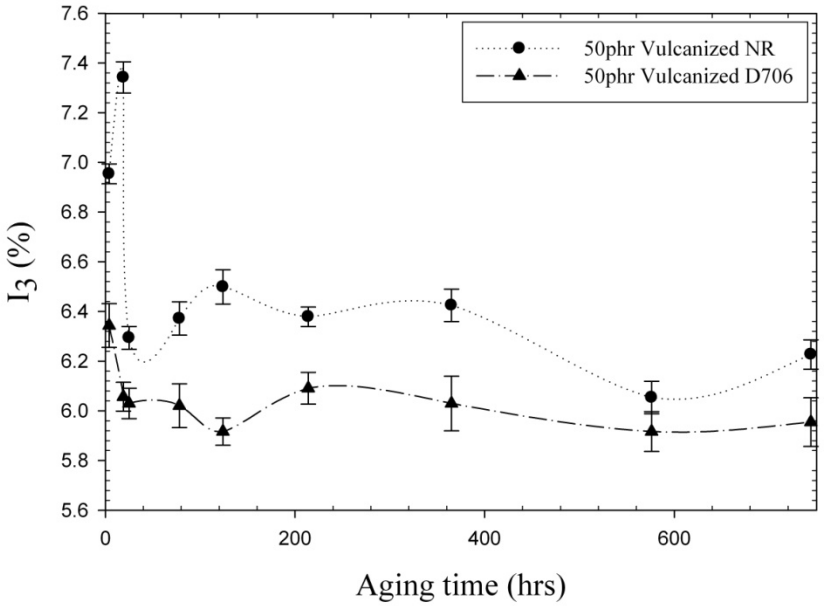

Figure 7.42 The o-Ps Intensity vs. Aging Time.

VII.7.2.3 Conclusions

As earlier indicated, aging is a heat driven process which can manifest itself either through physical changes in the sample or chemical changes. We have shown in these investigations that vulcanized NR samples have stable chain networks and can therefore resist aging at lower temperature, at least to our experimental aging time and conditions. Un-vulcanized samples however are weak and vulnerable to aging even at lower temperatures. This has been demonstrated above by the changes that occur in the o-Ps lifetime and intensity.

We have also observed that heat can favor the aligning of rubber chains in a more order manner leading to crystallization of the rubber at room temperature. We also found that the samples under heat underwent partly through oxidation process where the oxygen molecules attached themselves to the backbone of the unsaturated rubber chains. These oxygen molecules quench or reduce the o-Ps lifetime.

The results also demonstrate the differences in the property of natural rubber and synthetic rubber under extended aging time at high temperature. Whereas synthetic rubber cross-links are stable with temperature at least within the aging times investigated, natural rubber reverts easily, changing from a vulcanized sample to its original un-vulcanized gum state over a period of time, and then consequently degrading under extended heating time.

VII.8 Deformation of Natural Rubber Carbon Black Composites

Deformation measurements were done with an improvised system where a bench clamp was used to provide the deformation force. A groove with two steel pistons on both ends made of steel was fitted well in between the jaws of the bench clamp such that the pistons provided the deformation force whenever the handle was rotated. A vernier caliper was used to measure the change in length of the sample during deformation. The rubber sample was placed carefully between the jaws of the clamp and the ^{22}Na source was placed on the rubber and covered with an annealed copper plate. The source and copper plate did not move during deformation of the sample. The percentage strain E (%) was calculated according to the formula $E\ (\%) = ((l-l_o)/l_o)*100$, where l_o and l are the lengths of the sample before and after deformation respectively. The PALS measurements were begun after l reached a certain value under strain, then held constant during the measurements. We used pure vulcanized natural rubber and CB-filled natural rubber with different concentrations, in a per hundred rubber (phr) scale.

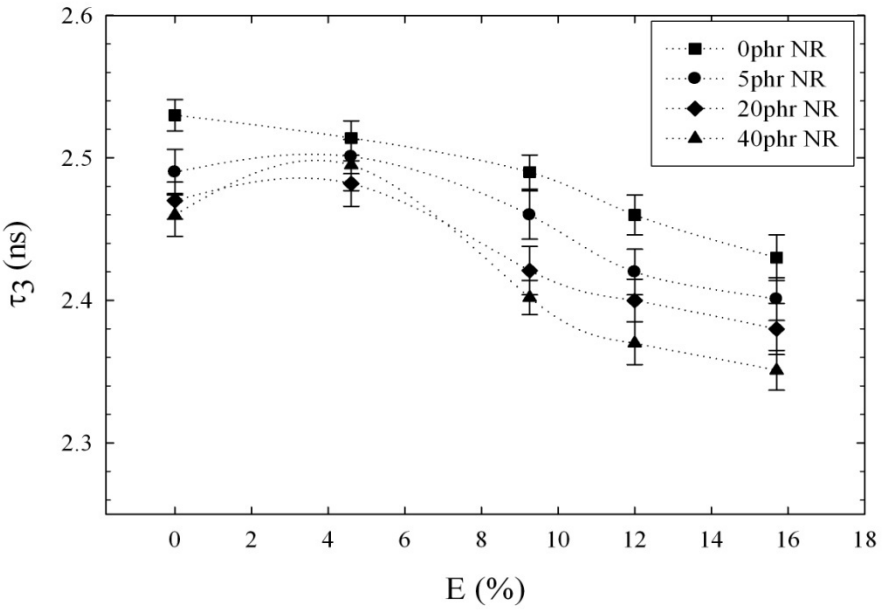

Figure 7.43 The o-Ps Lifetime vs. Strain

Figure 7.43 shows the changes in the o-Ps lifetime (τ_3) with deformation. The behavior of o-Ps lifetime seems different for different phr of CB. As the figure suggests, τ_3 decreased with strain for NR with no carbon black loading. We propose that deforming the rubber sample led to the aligning of the polymer chains along the applied force in a well ordered manner. If the Ps atom forms a bubble (s) in the un-compressed rubber network, then aligning the rubber chains reduces the size and the number, or possibly eliminates the bubble (s) from the rubber network, leaving only the pre-existing holes.

Samples with CB loadings, however, showed different behavior. There was first a slight increase in o-Ps lifetime with strain. We propose that CB impedes the aligning of polymer chains during the first stage of deformation. Due to the rigidity of the CB particles, polymer chain scission could have resulted, leading to the increase of o-Ps lifetime. On further deformation, the polymer chains were forced to align leading to the decrease in τ_3.

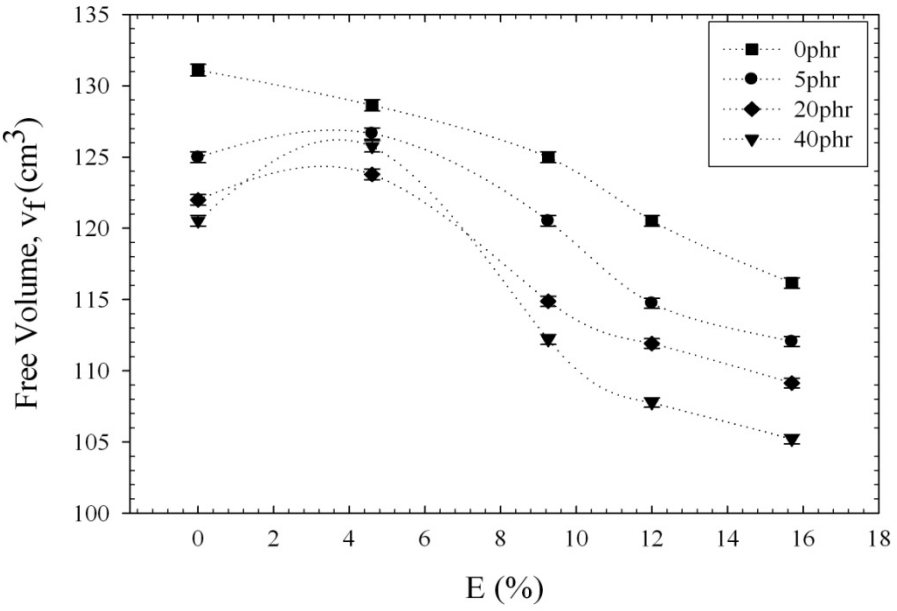

Figure 7.44 The Free Volume vs. Strain.

Another probable reason for the decrease in the free volume size is that CB brings about a structure in the network such that the rubber chains within the vicinity of CB aggregates are fixed and have the same shapes as the aggregates. The more CB concentration in the composite, the more ordered the network becomes. The annihilation due to the pickoff reaction in the pre-existing holes becomes more predominant than annihilation in the bubble would be. Deforming the sample composites thus leads to the change in the shape of the pre-existing free volume holes. The pick-off annihilation rate, which is proportional to the o-Ps lifetime, is dependent on the collision rate of the Ps with the walls of the hole. The smaller the hole the faster the annihilation rate and the shorter the o-Ps lifetime. Free volume shown in figure 7.44 behaves in essentially the same way as the o-Ps lifetime. Above 0 phr, the free volume increased slightly with initial strain and then decreased with further strain.

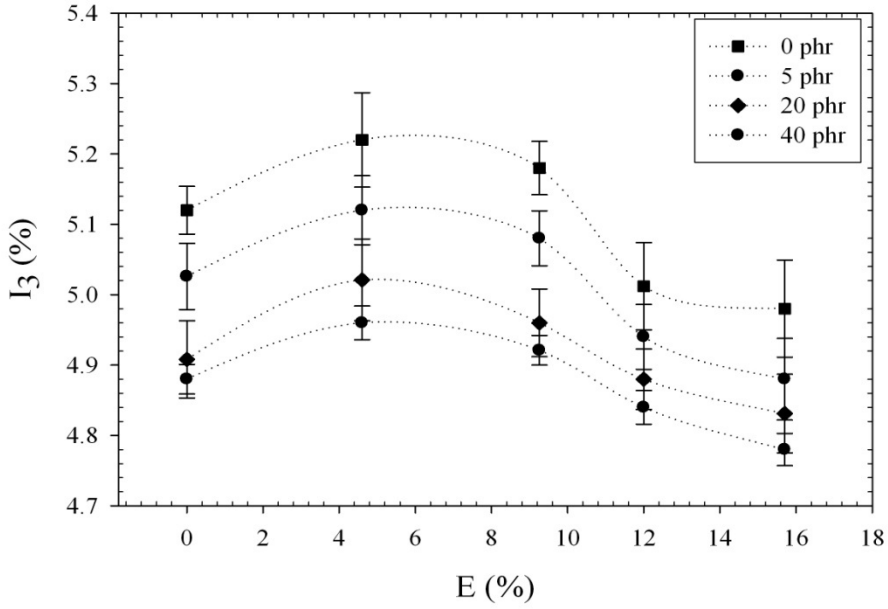

Figure 7.45 The o-Ps Intensity vs. Strain

I_3 did depend slightly on the deformation for sample without CB, as shown in figure 7.45. It first increased, reaching a yield point, then decreased. The behavior of I_3 can be understood by polymer chains unwinding during initial deformation, slightly increasing the number of free volume holes. On further deformation, the chains tend to align; reducing the number of available free volume holes and this was seen as a decrease in I_3 .

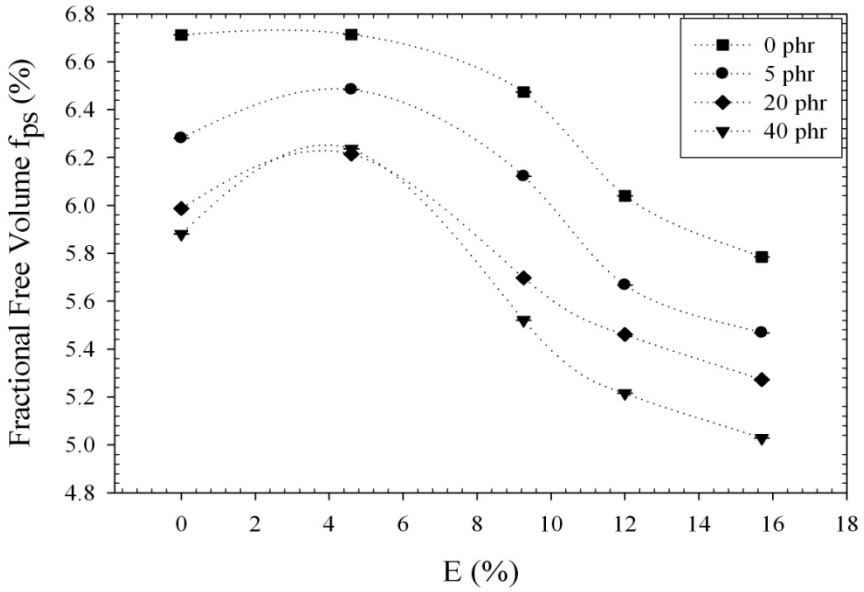

Figure 7.46 The Fractional Free Volume vs. Strain.

For samples with CB, there was slight increase in I_3, then a slight decrease to almost its original value. This slight increase could be interpreted as due to chain scission which could have also led to an increase in the number of free volume holes during deformation. CB is also a good conductor with high electron density and would thus favor direct annihilation with positrons rather than Ps formation.

The fractional free volume was plotted and shown in figure 7.46. At 0 phr, the fractional free volume initially remained constant initially with strain until up to 4.5% of strain was applied and then decreased with further strain. Conversely the free volume for 0 phr started to show some decrease with strain immediately. For samples with CB, however, the fractional free volume followed the same behavior as the free volume except that reaching yield point was delayed by about 1% of strain.

Another observation which can be drawn from these figures is that the higher the concentration of CB in the composite, the harder it is to deform the sample. This shows

the compactness and rigidity of the sample network brought about by the concentration of CB.

VII.8.1 Conclusions

These measurements show how PALS can detect the changes that occur in the polymer samples at a microscopic level. Natural rubber is far above its glass transition temperature and therefore behaves more like a liquid. The positron or Ps atom will therefore form a bubble in the NR sample. When deformed in the absence of CB, rubber chains align in an orderly fashion thereby reducing the size of the bubble, which depends on the nature and flexibility of the chains. When CB is added, the chains become less flexible; hence the annihilation by pickoff reaction dominates the annihilation in the bubble which increasingly becomes less probable with increasing CB concentrations. It also reveals the role played by CB as a filler in reinforcing polymers.

The results from these sections were presented at the ICPA conference in 2006 and a paper submitted for publication in Radiation Physics and Chemistry journal [67].

VIII. CONCLUSIONS AND FUTURE RESEARCH.

In performing this research there have been several significant contributions made to the scientific literature. These studies have helped us discriminate Natural Rubber from Synthetic Rubbers. We have been able to show at a microscopic level that NR has unstable molecular chains which reverse from vulcanized state to un-vulcanized gum state at high temperature. Synthetic rubbers on the other hand exhibit stable molecular chains at high temperatures, probably due to their high concentrations of pure elastomers in their chain.

We have also found that heat can induce crystallization in the rubber chain network. The most common type of rubber crystallization inducement is through strain, which has been studied in detail. In our investigation, we have found that when rubber is heated and allowed to cool slowly to room temperature, its chains can align themselves in an orderly fashion many times leading to crystal growths. Heat also favors oxidation of the rubber chains, hence causing their quick degradation.

In this work, we have also shown that deforming a polymer leads to the aligning of the polymer chains in a well ordered manner. CB impedes this aligning of the chains which could be another good reason apart from reinforcing the rubber why CB is added to the rubber used in tire manufacturing.

Results for o-Ps intensity and S parameter obtained from rubber samples interestingly exhibit a similar pattern as those of liquids, suggesting the formation of bubble void in the rubber network when positrons are injected in them. At room temperature, the rubbers are far above their glass transition temperature (T_g) and thus look more like a liquid than a rigid polymer. When carbon black is introduced in the rubber, the molecular chains

within the vicinity of CB are fixed, hence slow to move. They take the shape of the CB within their vicinity and possess some kind of structure. Away from the CB vicinity, the chains are still flexible and ready to move about as in the liquid state. So, we see a transition from more flexible liquid-like chains to more immobile chains as the CB concentrations increase. In this respect, the Ps atom would preferentially annihilate in the pre-existing free volume holes to the bubble formation. We should also point out here that CB is also an inhibitor of positronium formation.

We have also shown by using PAS the role sulfur plays in the vulcanization of rubber. Sulfur is believed to tie the rubber molecular chains together, forming cross-links with the chains restricting their motions. We found that the higher the sulfur concentrations in the network, the greater the cross-link density, hence the stiffer the rubber samples. The overall effect when the concentration of sulfur is higher in the chain network is the inhibition of the bubble formation. The Ps atom cannot squeeze itself in a stiffer polymer chain network to form the bubble.

In order to understand the nature and behavior of rubber and rubber-CB composites by PAS, we propose the continuation of the research in the following areas:

1. Depth profile study to investigate the homogeneity of the rubber-carbon black composites. Preliminary measurements with the Na-22 source (not reported here) have been inconclusive.
2. Develop a model that takes into account both the pre-existing free volume holes and the bubble formation.
3. Further study the rubber sample properties below or near their glass transition temperatures. Wang et al [44] [45] has measured lifetimes for a variety of

samples, but more work involving a comparison of the S parameter and o-Ps intensity for the rubbers below their glass transition temperature would be very interesting.

4. Extend the deformation measurements to stretching as well as compression. How about extending measurements to synthetic rubbers and different CBs?

In conclusion, an important part of my dissertation is the development of the Bubble model from the free volume model and the separation of the two depending on the nature and the state of the sample material. The Bubble model dominates the free volume model when the glass transition temperature of the sample material is much above the room temperature (experimental testing temperature). In this case, the sample is quite soft and flexible; hence the positron or the Ps atom can just dig its own cavity from which it will eventually annihilate. We have seen that this occurs in the liquids and the rubbers. Near or below glass transition temperature, the sample material is hard and immobile; hence the positron or Ps atom resides in the pre-existing free volume holes as opposed to forming the bubble. They will eventually annihilate in these free volume holes. This annihilation type is common in the more general polymers.

APPENDIX.

Tao-Eldrup Model

In order to interpret the parameters of PAL experiment as they relate to polymers, we look at a theoretical model, the Tao-Eldrup model [54], which gives the relationship between positronium lifetime and the free volumes hole size.

Let's consider a simple model in which the Ps particle is in a spherical well with radius R_0. We can express the potential as:

$$V(r) = 0 \quad \text{when } 0 < r < R_0$$

$$V(r) = \infty \quad \text{when } r > R_0 \tag{24}$$

the radial part of Schrodinger equation is determined by the equation

$$R_{kl}^{''} + \frac{2}{r} R_{kl}^{'} + (k^2 - \frac{l(l+1)}{r^2}) R_{kl} = 0 \tag{25}$$

where $k = \sqrt{2mE}/\hbar$

For ground state $l = 0$, so the above radial function can be written as:

$$\frac{d^2(rR_{k0})}{dr^2} + k^2 r R_{k0} = 0 \tag{26}$$

with the boundary conditions:

$$rR_{k0}(r)\,|_{r=0} = 0 \tag{27}$$

$$rR_{k0}(r)\,|_{r=R_0} = 0 \tag{28}$$

So, the solution can be obtained as:

$$rR_{k0} = A \sin kr \quad (0 \le r \le R_0) \tag{29}$$

$rR_{k0} = 0$ (Somewhere else)

(30)

By using boundary condition (13), we get,

$$kR_0 = n\pi \qquad (n = 1, 2, 3 \ldots) \tag{31}$$

For the ground state (n = 0), we have $k = \frac{\pi}{R_0}$, so,

$$R_{k_0 0}(r) = A\sin(\pi r / R_0)/r \tag{32}$$

By using normalization condition:

$$\int_0^{R_0} [R_{k0}]^2 r^2 dr = 1 \tag{38}$$

We can obtain normalization constant:

$$A = \sqrt{\frac{2}{R_0}} \tag{33}$$

Finally, the ground state wave function for Ps is:

$$\Phi_{Ps} = \sqrt{\frac{2}{R_0}} \frac{\sin(\pi r / R_0)}{r} \quad (0 \leq r \leq R_0) \tag{34}$$

$$\Phi_{Ps} = 0 \qquad \text{(Somewhere else)} \tag{35}$$

The calculation of the annihilation rate needs the electron density. Instead of doing a calculation of electron density, Tao and Eldrup assume that inside the wall there is a homogeneous electron layer with a thickness $\Delta R = R_0 - R$. So, the probability of Ps in the ground state inside the electron layer is given by:

$$\text{Probability} = \int_{R}^{R_0} |\Phi(r)|^2 \, r^2 dr$$

$$= 1 - \frac{R}{R_0} + \frac{1}{2\pi}\sin(\frac{2\pi R}{R_0}) \tag{36}$$

Assume the annihilation rate of o-Ps inside the electron layer is $2\,ns^{-1}$, which is close to the pick off annihilation rate of Ps [51]. So the o-Ps annihilation rate as a function of free-volume radius R is given by

$$\lambda = 2P = 2[1 - \frac{R}{R_0} + \frac{1}{2\pi}\sin(\frac{2\pi R}{R_0})] \tag{37}$$

Here, P is the probability of Ps in the ground state inside the electron layer (from R to R_0). In the above equation, $R_0 = R + \Delta R$, where ΔR is an empirical parameter, which is determined by fitting the observed τ_3 with the known hole and cavity sizes in molecular substrates [51] [52]. The best-fitted value of ΔR for all known data has been found to be $1.656\,\mathring{A}$. The above function is the foundation for determining free-volume hole size by using PAL. So, the Tao-Eldrup equation is given by:

$$\tau = \frac{1}{2}[1 - \frac{R}{R_0} + \frac{1}{2\pi}\sin(\frac{2\pi R}{R_0})]^{-1} \tag{38}$$

where τ is o-Ps lifetime, R_0 is free-volume hole size and R is given by $R = R_0 - 1.656\,\mathring{A}$.

Although the above equation is based on a crude model of the particle-in-a-

spherical-box, a more extensive theoretical development [54] based on a finite potential shows that the above equation is still valid and most convenient for practical applications at good accuracy as long as the empirical parameter (i.e., electron layer thickness = $1.656\,\overset{o}{\text{A}}$) is well fitted to the known cavity radii and the measured o-Ps lifetimes.

Knowing R, one can calculate the free volume hole by:

$$v_f = \frac{4\pi R^3}{3} \tag{39}$$

GLOSSARY

-A-

ACAR. Angular Correlation of Annihilation Radiation. This is a Positron annihilation techniques where the angle between the annihilating gamma pairs are measured.

ASTM D3191. American Society for Testing and Materials D3191**.** This is the agreed recipe for the mixing and preparation of rubber.

-D-

D706. Duradene 706**.** This is a synthetic rubber.

DBS. Doppler Broadening Spectroscopy. One of the techniques in Positron Annihilation Spectroscopy which involves measuring the positron annihilation line shape, which directly corresponds to the momentum distribution of the electron-positron pairs and Doppler broadened at the annihilation site.

-C-

CAARI. Conference on the Application of Accelerators in Research and Industry. Conference that brings together scientist from all over the world who use particle accelerators in their research and industrial applications.

CB. Carbon Black. Carbon black is an industrial product obtained by partial combustion or thermal decomposition of hydrocarbon compounds used in reinforcing rubber.

CDBP . Crushed Dibutyl Phthalate**.** This is a measure of the degree of irregularity of the carbon black units or the development of branching due to the aggregation of primary particles and the asymmetry of the aggregates.

CFDD. Constant Fractional Differentail Discriminator**.** This is the component in lifetime apparatus which is used in selecting the start and stop signals during

lifetime measurements.

-F-

FTIR. Fourier Transform Infrared Spectroscopy. This is an analytical technique used to identify organic (and in some cases inorganic) materials. This technique measures the absorption of various infrared light wavelengths by the material of interest. These infrared absorption bands identify specific molecular components and structures.

-I-

ICPA. International Conference on Positron Annihilation. This is a conference that brings people around the world with an aim of discussing about the progress in fundamental aspects of positron and positronium physics and chemistry, applications of positron annihilation techniques to material science and industry, and new developments in experimental techniques.

-L-

LT. Lifetime

-M-

MCA. Multichannel Analyzer**.** This is the component in the positron annihilation spectroscopy setup that builds the spectrum for final analysis.

MBTS. Mercaptobenzothiazole Sulfanimide**.** This is one of the accelerators used to reduce the vulcanization time (cure time) by increasing the rate of vulcanization.

-N-

N330. This is defines the type of carbon black grade used.

N_2SA. Nitrogen Surface Area**.** It is a measure of the carbon black particle sizes**.** A small particle-size carbon black will have a high surface area accessible for

interaction with rubber molecules per unit weight.

NR. Natural Rubber

-O-

o-P. ortho-Positronium**.** The is the long living part of the Positronium atom with a lifetime of about 142 ns.

-P-

PAL. Positron Annihilation Lifetime**.** This is one of the techniques of Positron Annihilation Spectroscopy that involves measuring the lifetime of a positron in a material medium.

PAS. Positron Annihilation Spectrocopy**.** This is a spectroscopic tool that uses positron, an anti-electron as its probe in trying to understand the nature and defects in materials.

Ps. Positronium**.** This a temporary atom formed by interaction between an electron and a positron.

p-P. para-Postronium**.** This is the short living component of the positronium, with a lifetime of about 125 ps.

-S-

SBR. Styrene-Butadiene Rubber**.** This is a synthetic rubber.

SEM. Scanning Electron Microscopy**.** This is a spectroscopic tool that uses electron microscope that is capable of producing high resolution images of a sample surface.

Sn-SSBR. Solution Styrene-Butadiene Rubber. This is a synthetic rubber.

-T-

TEM. Transmission Electron Microscope**.** This is an imaging technique whereby a beam of electrons is focused onto a specimen causing an enlarged version to appear on a fluorescent screen or layer of photographic film, or to be detected by some special camera.

-Z-

ZnO. Zinc Oxide. This is an activator used in increasing vulcanization rates and improving the final product's properties of rubber.

REFERENCES.

[1] A. Dupasqueir, P. A. Mills Eds; *Positron Spectroscopy of Solids, Proceedings of the international School of Physics "Enrico Fermi ", Course CXXV, Varenna, Italy, July 6-16, 1993*; IOOS Press: Amsterdam, (1995).

[2] D.M.Shrader and Y.C.Jean; Positron and Positronium chemistry; Elsevier (1988).

[3] M. Maurice, *Rubber Technology*, Van Nostrand Reinhold Inc., New York (1987).

[4] J.B. Donnet, Carbon *Black*: Science and Technology 2nd ed., New York, (1993).

[5] M.O .Gerspacher, Rubber Chemical and Technology, **69** (1996) 569.

[6] A.J. Kovacs, Advanced Polymer Science, **3** (1963)394.

[7] L.C.E Struik, *Physical Aging in Amorphous Polymers and other materials*. Elsevier Sci, Amsterdam-Oxford NY,(1978).

[8] M. H. Cohen and D. Turnbull; J. Chem. Phys. **31** (1959) 1164.

[9] D.Turnbull and M. H. Cohen, J.Chem. Phys. **34** (1961) 120.

[10] T.A. Litovitz and P. Macedo, " *Proceedings International Conference on Physics of Non-Crystalline solids*", J.A. Prins, Ed., North-Holland, Amsterdam, 220 (1965).

[11] J. T. South, *Dissertation*; Virginia Polytechnic Institute and State University (2001).

[12] C. Huang, R. Fan and Y. Zhang, "Effect of Aging on NR Vulcanizates," He Cheng Xiang Jiao Gong Ye: China Synthetic Rubber Industry, **23**, (2000 288.

[13] L. I. Lyubchanskaya, A. S. Kuzminski "The degradation of main chains and crosslinks in the aging of vulcanizates," Doklady Akad. Nauk SSSR, **135** (1960) 1438.

[14] E.J. Blackman and E.B McCall "*Relationship between the Structures of Natural*

Rubber Vulcanizates and Their Thermal and Oxidative Aging." Division of Rubber Chemistry, Rubber Chemistry and Technology, Buffalo, New York, (1969).

[15] J. M. Sloan "Reversion Studies of Natural Rubber on Reversion Behavior," U.S. Army Materials Technology Laboratory: Polymer Research Branch, (1992).

[16] G. M. Bristow "Influence of Grade of Natural Rubber on Reversion Behavior," Journal of Natural Rubber Research, **6 (**1991)137.

[17] G. R Mitchell, D.J Brown and A. H Windle "The interpretation of Orientation-Strain Relationships in Rubbers and Thermoplastic," *Polymer*, **36** (1985) 1755.

[18] G. R Mitchell "Orientation-Strain Behavior of Crosslinked Rubbers," British Polymer Journal, **17**(1985)111.

[19] A. Dubault, B. Delocke and Herz J. "Effect of crosslinking Density on the Orientation Order Generated in Strained Networks: A Deuterium Magnetic Resonance Study", Polymer; **25** (1984)1405.

[20] B. Amram, L. Bokobza, J. P Queslel, Monnerie L. "Fourier- Transform Infra-Red Dichroism Study of Molecular Orientation in Synthetic High Cis-1, 4-Polyisoprene and in Natural Rubber," Polymer, **27** (1986)877.

[21] J. P.Queslel, L. Monnerie, B. Erman. "Characterization of Segmental Orientation in Stretched Rubbery Networks by the Stationary Fluorescence Polarization Technique," Journal of Macromolecular Science and Chemistry A, **26** (1989)93.

[22] P.Munk and T.M. Aminabhavi, *Introduction to macromolecular science* 2nd ed, Wiley, New York (2002).

[23] G.S. Whitby in The chemistry and Technology of Rubber, C.C. Davis, ed., J.T Blake, assoc. ed., Reinhold, New York (1937).

[24] C. Neogi, S. P Basu and A. K Bhowmick. "Analysis of Rubber-Filler Interaction at High Temperature by Using Strain Amplification Factor," Plastics and Rubber Processing and Applications, **12**(1989)147.

[25] M. J Wang "Effect of Polymer-Filler and Filler-Filler Interactions on Dynamic Properties of Filled Vulcanizates" Rubber Chemistry and Technology, **71**, (1998)520.

[26] T. Ungár, J. Gubicza, G. Ribárik, C. Pantea and T. W. Zerda; Carbon **40** (2002) 929.

[27] P.E.Mallon, Y.C.Jean and D.M.Shrader; *Positron and Positronium chemistry*; World Scientific (2003).

[28] B. H. Stuart, *Polymer Analysis*, Wiley, New York (2002).

[29] A. H. Fawcett, *Polymer Spectroscopy*, Wiley, New York (1997).

[30] J.B. Donnet and A. Voet, *Carbon Black*; Physics, Chemistry and Elastomer reinforcement, Dekker, New York (1976)

[31] S. Brunauer, P.H Emmett and E. Teller, J. America Chem. Soc., **60** (1938) 308.

[32] A. J Marzocca , S. Cerveny, W. Salgueiro, A. Somoza, L. Gonzalez; Phys Rev E **65** (2002)021801.

[33] W. Salguiro, A. Marzocaa, A. Somoza, G. Consolati, S. Cerveny, F. Quasso and S. Goyanes; Polymer, **45** (2004)6037.

[34] R.Strithawatpong, Z.L. Peng, B.G. Olson, A.M. Jamieson, R. Simha, J.D. Mcgervey, T.R. Maier, A.F. Halasa, H. Ishida; J. Polym Sc B Polym Phys, **37** (1999) 2754.

[35] S.S. Choi; Bull. Korean Chem. Soc. **21** (2000) 6.

[36] Y.C. Jean, H. Nakanishi, L.Y.Hao and T.C. Sandreczki; Phys. Rev. B; **42**(1990)

9705.

[37] G.Dlubek, T.Lupke, H.M. Fretwell, M.A Alam, A. Wutzler and H.J. Radusch, Acta Polymer; **49** (1998) 236.

[38] Y.Y. Wang, H Nakanishi, Y.C.Jean, and T.C. Sandreczki; J. Polym. Sci. Part B: Polymer Physics, **28** (2003)1431.

[39] M.Mohsen, M.H. Abd-El Salam, A. Ashry, A. Ismail, H. Ismail; Polym Degrad & Stab. **87**(2005) 381.

[40] C.A Quarles, J.M.Urban, M.Gerspacher, L.Nikiel and M.E Semaan; Material Science Forum, **363**(2001) 343.

[41] J.M. Urban, C.A. Quarles, J. Appl. Phy. **86** (1999) 259.

[42] M.E. Semaan, C.A. Quarles and L. Nikiel; Polym Degrad Stab **75** (2002)259.

[43] M.E. Semaan, L. Nikiel, C.A. Quarles; Carbon **39**(2001)1379.

[44] J. Wang, C.A Quarles, Radiat Phys. Chem., **68** (2003) 527.

[45] J. Wang, V.O.Jobando, and C.A.Quarles; Nuclear Instruments and Methods in Physics Research B; **241**(2005) 271.

[46] R.A. Ferrel, Phys. Rev. **110**(1958)1355.

[47] R.S. Yu, T. Suzuki, Y. Ito, N. Djourelove, K. Kondo and V. Shantarovich; Chem. Phys. Letters, **406**(2005) 101.

[48] J. Kansy; Nucl. Instr. and Meth. A **374** (1996) 235.

[49] C.D. Anderson, *Phys. Rev* **43** (1933).

[50] W. Brandt, S. Berko and W.W. Walker, Phys. Rev. **112** (1960)1289.

[51] Y.C. Jean: Nucl. Inst. Meth, *B*, **56** (1991) 615.

[52] H. Nakanishi, Y.C. Jean, E.G. Smith, T.C.Sandreczki: J.Pol. Sc.Part B; **27** (1989)

1419.

[53] A. Ore and J.L. Powell, Phys. Rev. **75**(1949) 1696.

[54] O.E. Mogensen, J. Chem. Phys. **60**(1974) 998.

[55] T. Mukherjee, B.N. Ganguly, and B. Dutta-Roy, J. Chem. Phys., **107**(1997)7467.

[56] K.Sato, K.Ito, K. Hirata, R.S. Yu, Y. Kobayashi, Phys. Rev. B: **71** (2005) 012201.

[57] S.J.Tao, J. Chem. Phys. **56**, 5499 (1972)

[58] N. S. Schneider, J. A. Moseman and N. H. Sung; J. Polym. Sci. Part B: Polym Phys, **32** (1994) 491

[59] J. M. Urban, *Dissertation*; TCU Physics Dept. (1996).

[60] T. Suzuki, T. Miura, Y. Oki, M. Numajiri, K. Kondo and Y. Ito; Radiat. Phys. Chem **45** (1995) 657.

[61] Z. L. Peng Z.L, B. G. Olson, J. D. McGervey, A.M. Jamieson; Polymer, **40** (1999) 3033

[62] X.S.Li, M.C. Boyce; J. Polym. Sci. Part B: Polym. Phys, **31** (1993) 869.

[63] C.Qi, W. Wei, Y. Wu, S. Zhang, W. Haijun, H. Li, T. Wang, F. Yan, J. Polym. Sci. Part B: Polym. Phys., **38**(2000) 435.

[64] C.A. Quarles, V.O. Jobando and P. Arpin; Nuclear Instruments and Methods in Physics Research, accepted.

[65] V.O. Jobando and C.A. Quarles, Rad. Phys. Chem, submitted.

[66] V.O. Jobando and C.A. Quarles, Rad. Phys. Chem, submitted.

[67] V.O. Jobando and C.A. Quarles, Rad. Phys. Chem, submitted.

VITA

Vincent Okello Jobando

Vincent Okello Jobando was born on September 12th 1975 in Migori, Kenya. He is the son of the late Mr. Yuda Jobando and the late Mrs. Loice Akuno Jobando. He graduated from Mbeji Academy in 1993 after successful completion of Kenya Certificate of Secondary Education exams.

From 1995-1999, he was a student at Moi University (Maseno Campus) where he majored in Physics and minored in Mathematics. He graduated with an upper class honors in December 1999 after which he became a High School teacher in his local home town. After less than a year of teaching, he received a graduate assistantship award to study his Master of Science degree in Physics at Miami University, Ohio USA. He graduated with his M.S in August 2002.

Upon graduation from Miami University, he received two teaching assistantship awards from Oklahoma State University and Texas Christian University. He opted for Texas Christian University in Fort Worth, TX USA where he also started his doctorate program in physics.

He is married to Mary Okello and they have a five year old daughter, Perpetua Leanne Okello.

ABSTRACT

POSITRON ANNIHILATION SPECTROSCOPY STUDIES OF
RUBBER-CARBON BLACKCOMPOSITES

by Vincent Okello Jobando, PhD., 2006
Department of Physics
Texas Christian University
Dissertation Advisor: Dr. C.A. Quarles, Professor of Physics

The focus of this research was to use Positron Annihilation Spectroscopy (PAS) to investigate the response of rubber and rubber-carbon black composites subjected to different physical conditions. The work examined the effect of deforming rubber and rubber filled with carbon black. The results showed that deformation of the rubber depends on whether the sample is filled with carbon black (CB) or not. CB, we propose impedes the aligning of the rubber chains during deformation.

Aging of rubber was done and natural rubber was found to exhibit reversion property of its chains from a vulcanized state to un-vulcanized gum state as opposed to synthetic rubbers. This shows how vulnerable the natural rubber chains are at high temperature. We also found that heat can induce crystallization in the rubber chain network. The most common type of rubber crystallization inducement is through strain, which has been studied in detail. In our investigation, we have found that when rubber is heated and allowed to cool slowly to room temperature, its chains can align themselves in an orderly fashion many times leading to crystal growths. Heat also favors oxidation of the rubber chains, hence causing their quick degradation

We studied the effect of sulfur in the cross-linking of rubber. We found that during vulcanization, sulfur cross-links rubber chains by tying them together in a network like structure reducing the chains' mobility.

The work also explored the positronium formation in liquids and some common polymers then compared the results with those found from rubber. It was found that Ps formation depends on the nature of the liquid. We found that the results for rubber were similar to those of liquids and concluded that rubber behaves more like a liquid. At room temperature, rubber is far away from its glass transition temperature hence has soft and flexible chains. Ps atom can thus dig itself a cavity within the rubber chains and live longer in it. This explanation was explored through the bubble model.